with the distribution of banded ironstone and komatiitic basalt. It agrees with a small scale geochemical anomaly as does a low resistivity zone near point D-4-45, where banded ironstone occurs.

2-3-3 Discussion

Seven, SIP survey lines were planned, for selection as a result of comprehensive investigation of the CSAMT survey and geological and geochemical prospecting results. They are described as follows.

Area D 1

(1) A 1.0 km survey line crossing the low resistivity zone around survey point D-30-9:

The distribution of the low resistivity zone agrees with the geochemical anomaly on the surface, and mineralized zones in serpentine are expected in shallow to deep parts.

(2) A 1.0 km survey line crossing the low resistivity zone around point D-37-6:

There is an anomaly of the first principal component of geochemical exploration near survey point C-38-6. Lochness shaft occurs near point C-39-9. It is said to prospect cassiterite containing pegmatite, but no sign of minerals is noticed on the surface. The low resistivity zone extends in a NNW direction into the neighborhood of point D-33-6 with repeated expansion and contraction. The regional geology is associated with sedimentary rocks and serpentine, and mineralized zones in the deep serpentine are expected.

Area D 2

(3) A 1.0 km survey line crossing the low resistivity zone around survey point D-7-15:

Although results suggest the effect of clay-including zones in the

shallow alluvium, mineralized zones are expected in the deep part of the western serpentine rock.

(4) A 1.0 km survey line crossing the low resistivity zone near survey point D-4-9:

This low resistivity zone extends to the deep part of the resistivity structure plan with D-3-12 at the center. Mineralized zones in the serpentine rock are expected.

Area D 3

(5) A 1.0 km survey line crossing the low resistivity zone near survey point D-9-45:

(6) A 1.0 km survey line corssing the low resistivity zone near survey point D-7-39:

The low resistivity zones in (5) and (6) are separate at 125 m depth, but unite below 225 m and extend over a wide area. It includes the Tynan mineralization zone in serpentine rock which has intruded into sedimentary rocks, banded ironstone and komatiitic basalt. The same quality pyroclastic rock occurs near survey points D-10-39 to D-9-42, and the mineralization zone is therefore thought to extend over a very wide range.

(7) A 1.8 km survey line crossing over two low resistivity zones with survey points D-3-33 and D-3-45 at the center:

Surface geology of the low resistivity zone near survey point D-3-33 is banded ironstone, but a deeper concealed extension of serpentine rock is expected along with mineralized zones. The low resistivity zone near D-3-45 is banded ironstone on the surface, but mineralized zone are expected deeper down.

A, B, C, and D SIP method survey lines described in the next chapter were determined as a result of the above discussion and order of priority.

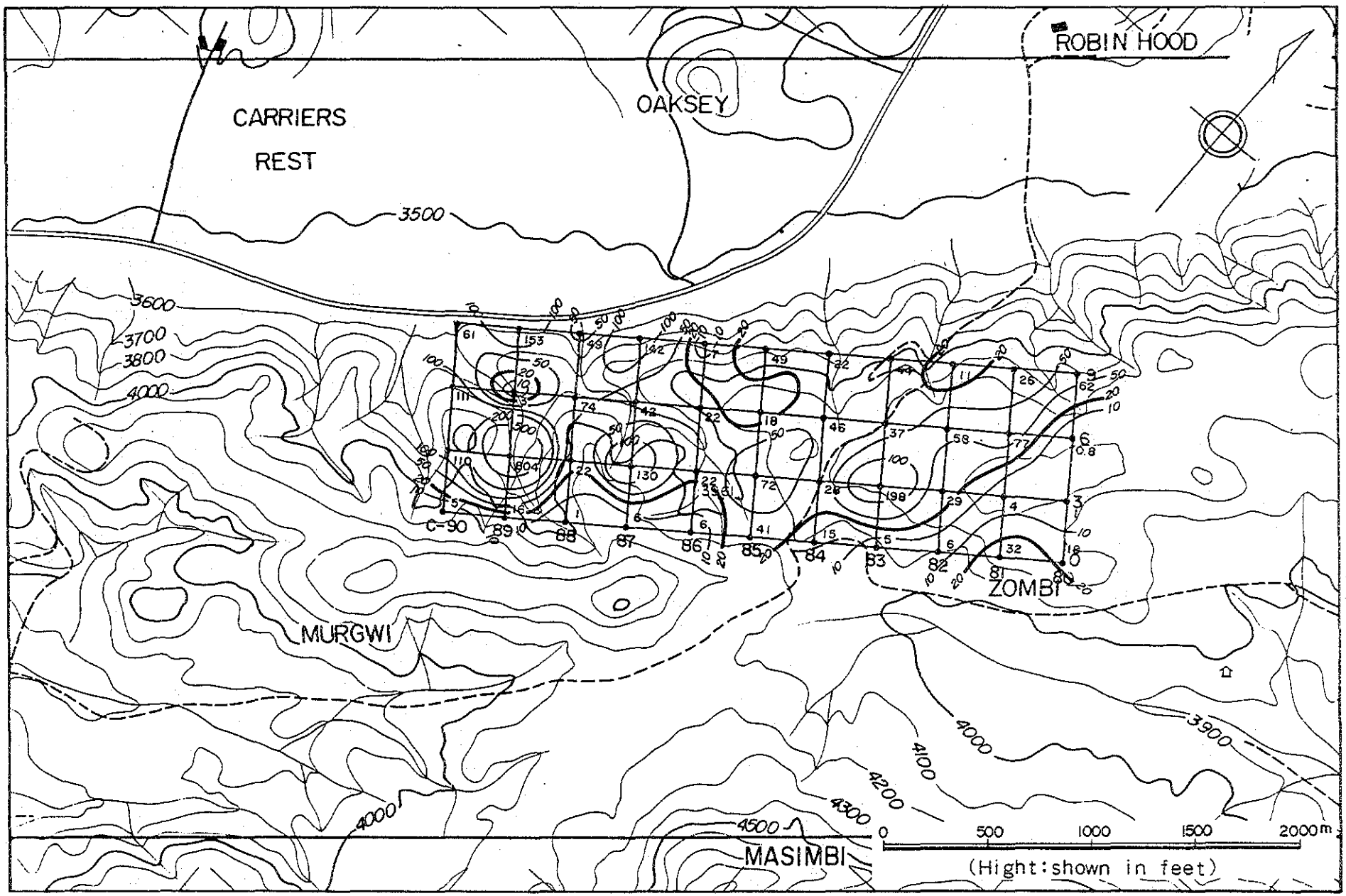

Fig. Ⅱ-7 Plan of Apparent Resistivity (Area C, 1024Hz) unit:Ω-m

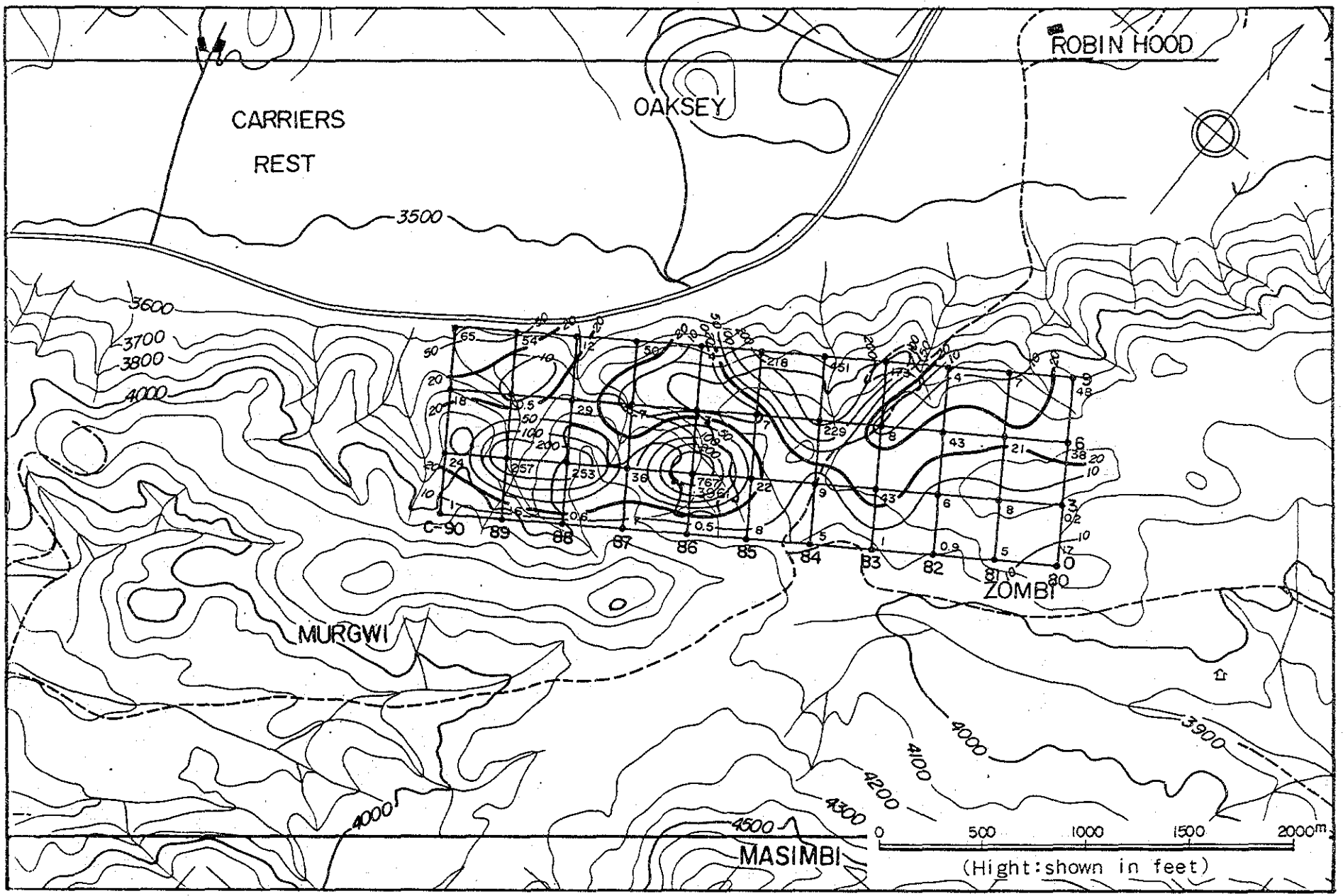

Fig. Ⅱ-8 Plan of Apparent Resistivity (Area C, 256Hz) unit:Ω-m

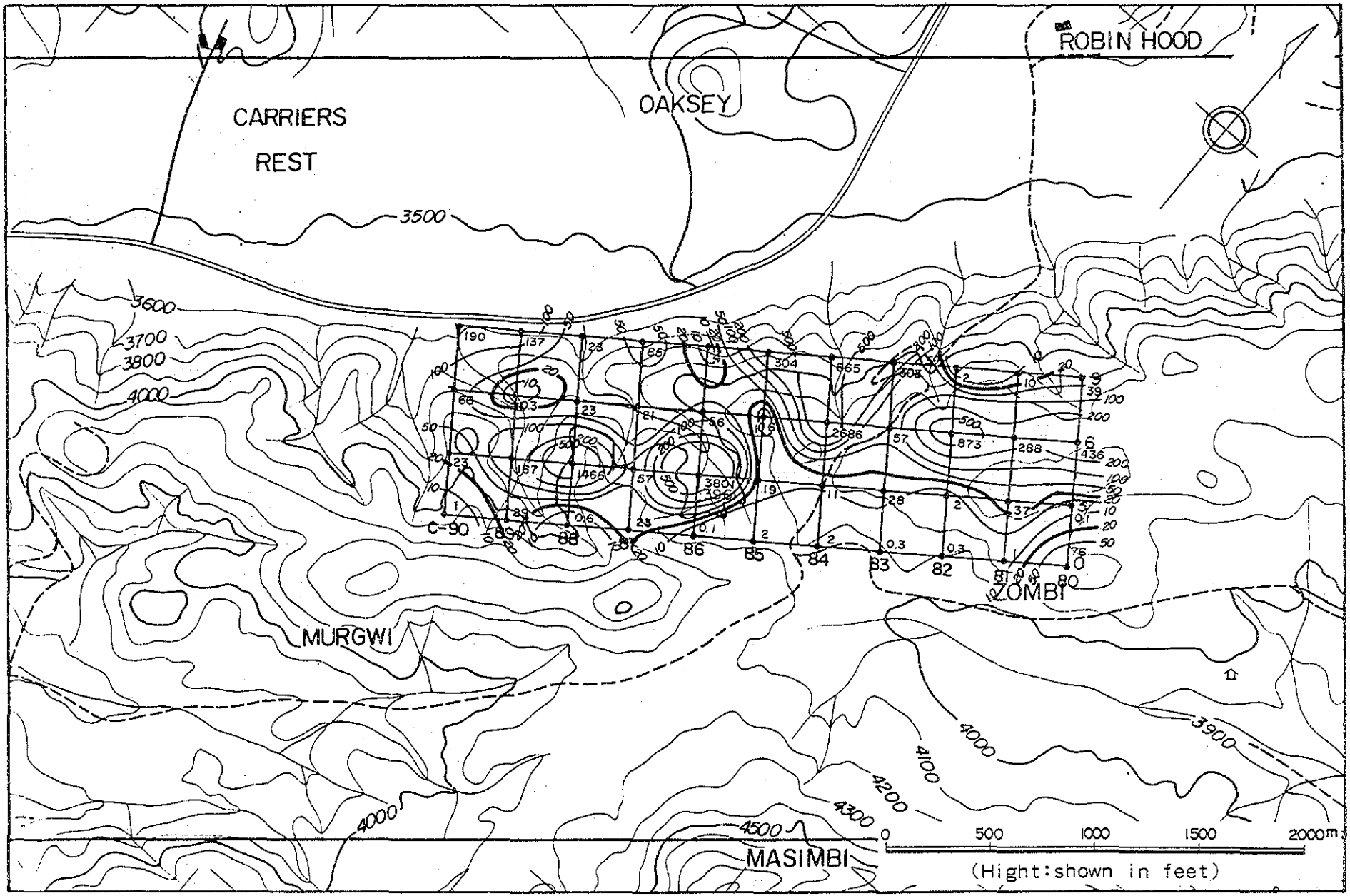

Fig. Ⅱ-9 Plan of Apparent Resistivity (Area C, 64Hz) unit:Ω-m

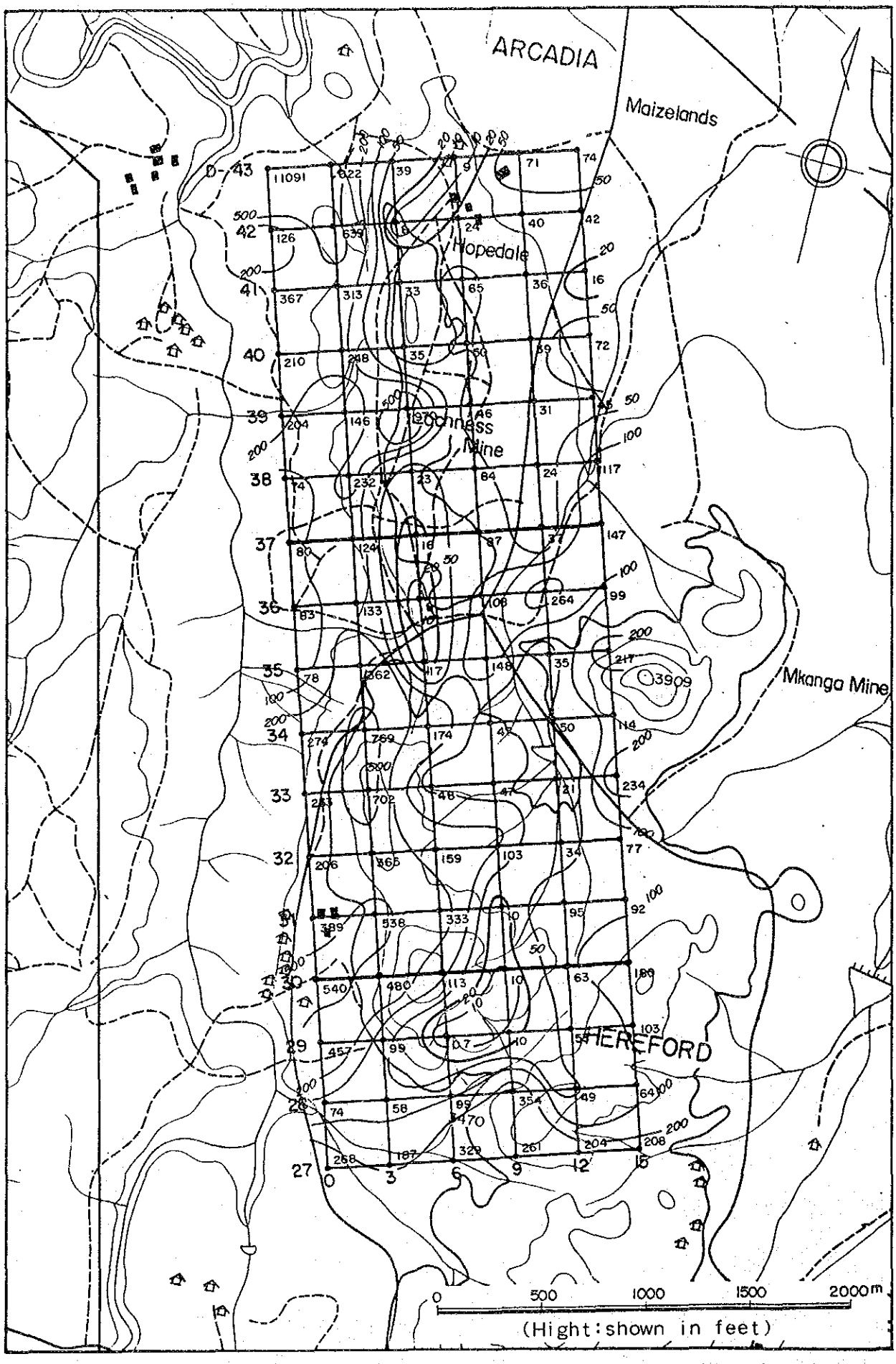

Fig. Ⅱ-10 Plan of Apparent Resistivity (Area D1, 1024Hz) unit:Ω-m

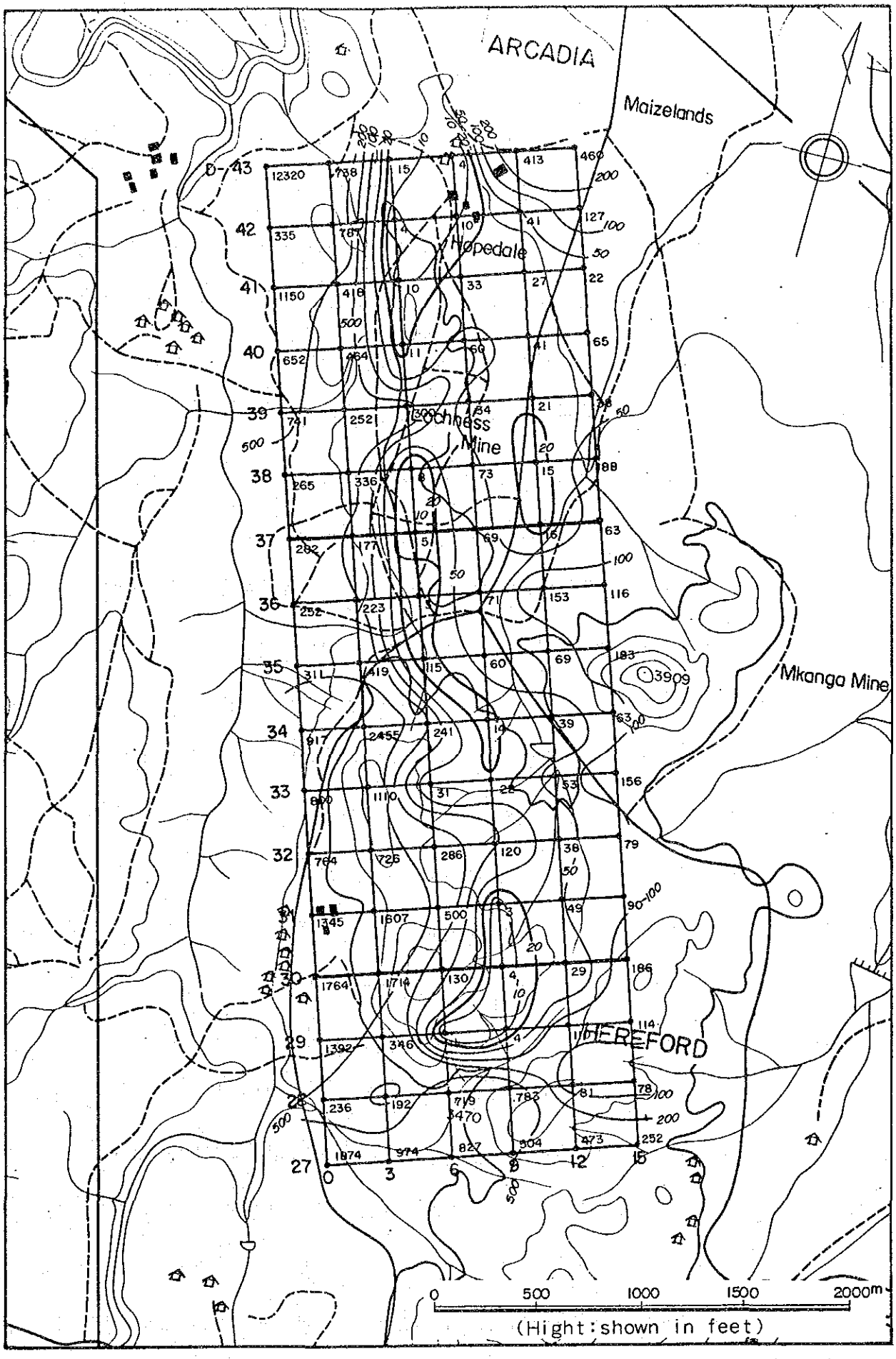

Fig. II-11 Plan of Apparent Resistivity (Area D1, 256Hz) unit:Ω-m

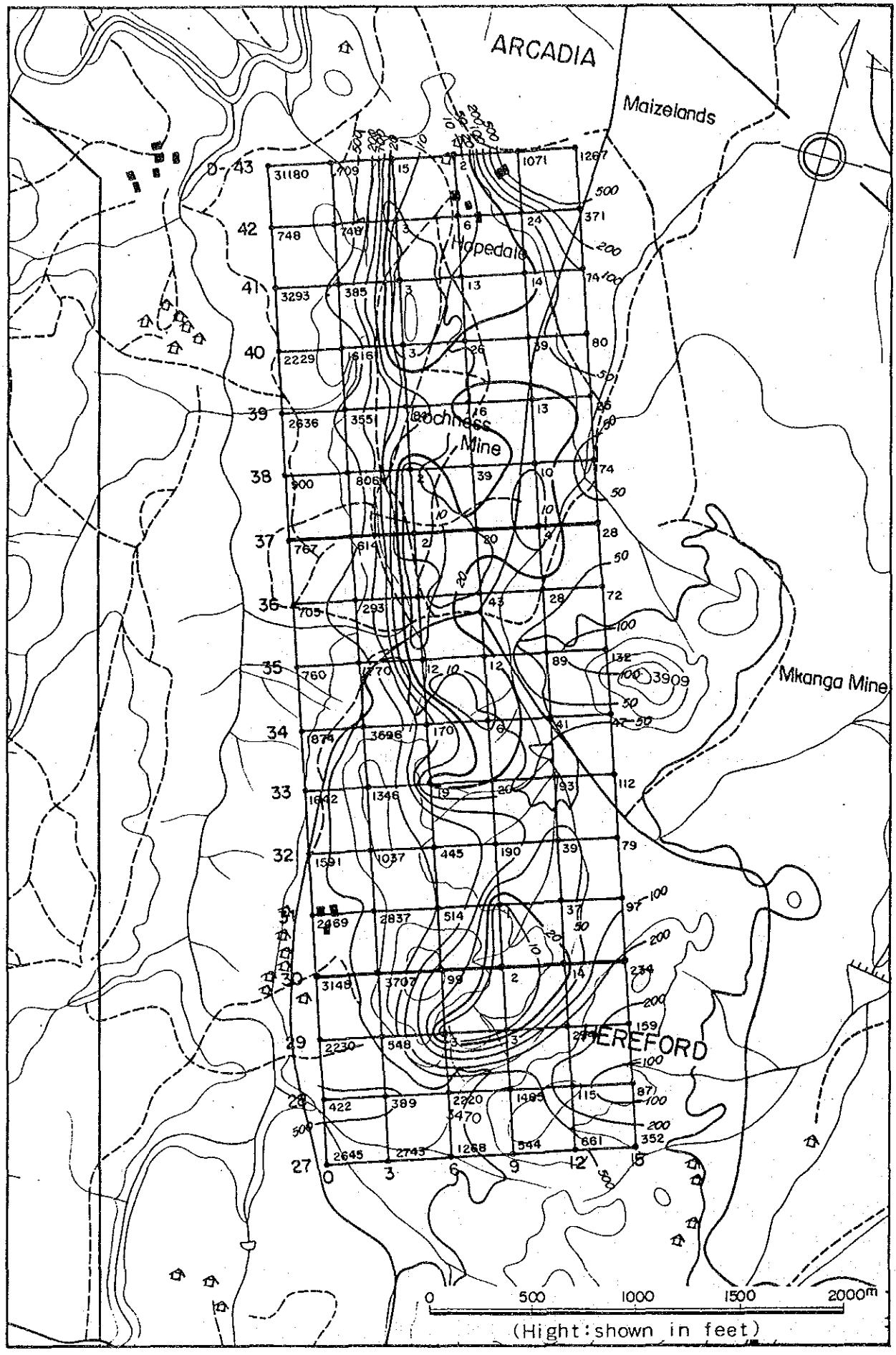

Fig. II-12 Plan of Apparent Resistivity (Area D1, 64Hz) unit:Ω-m

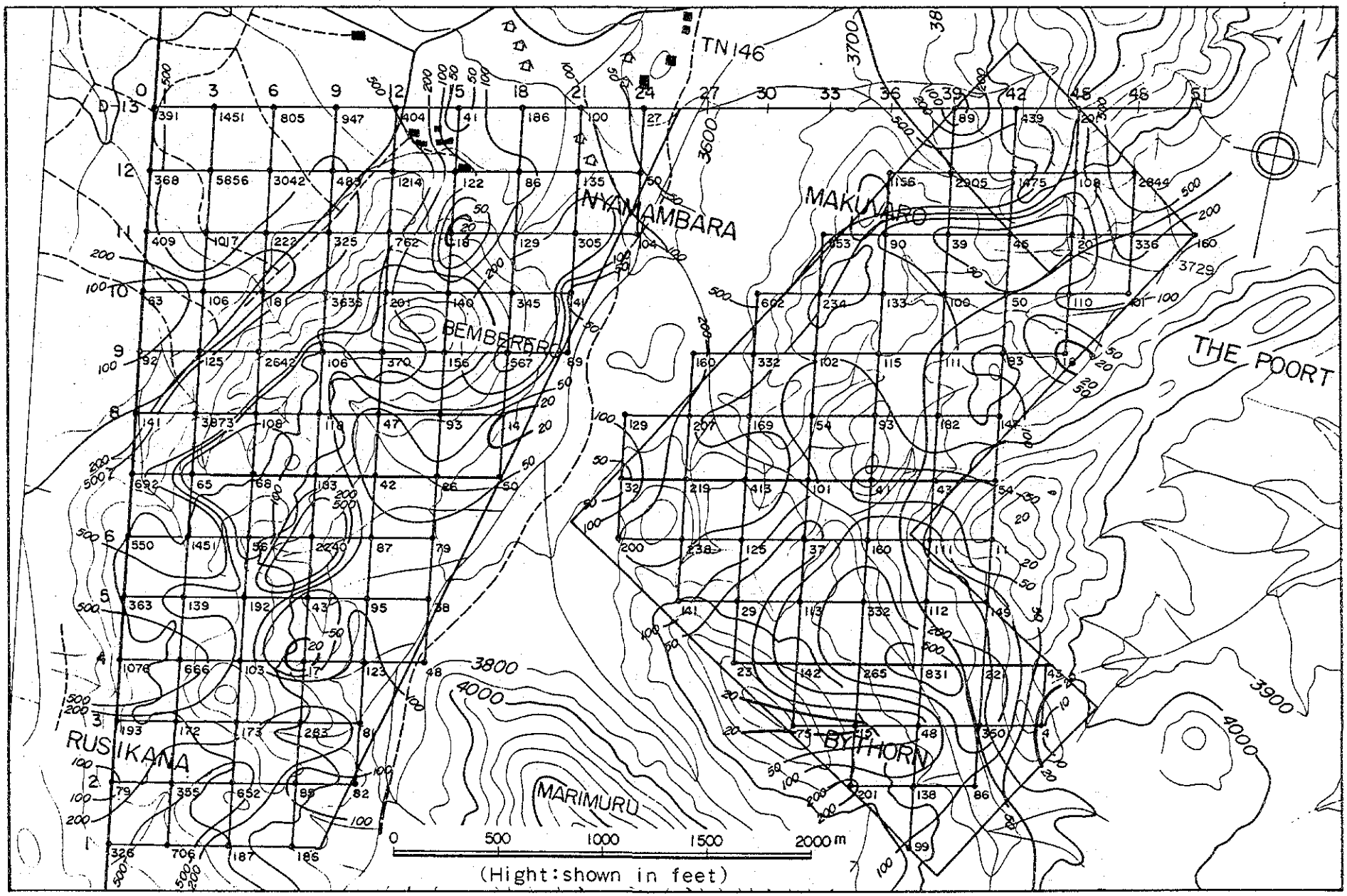

Fig. Ⅱ-13 Plan of Apparent Resistivity (Area D2·D3, 1024Hz) unit:Ω-m

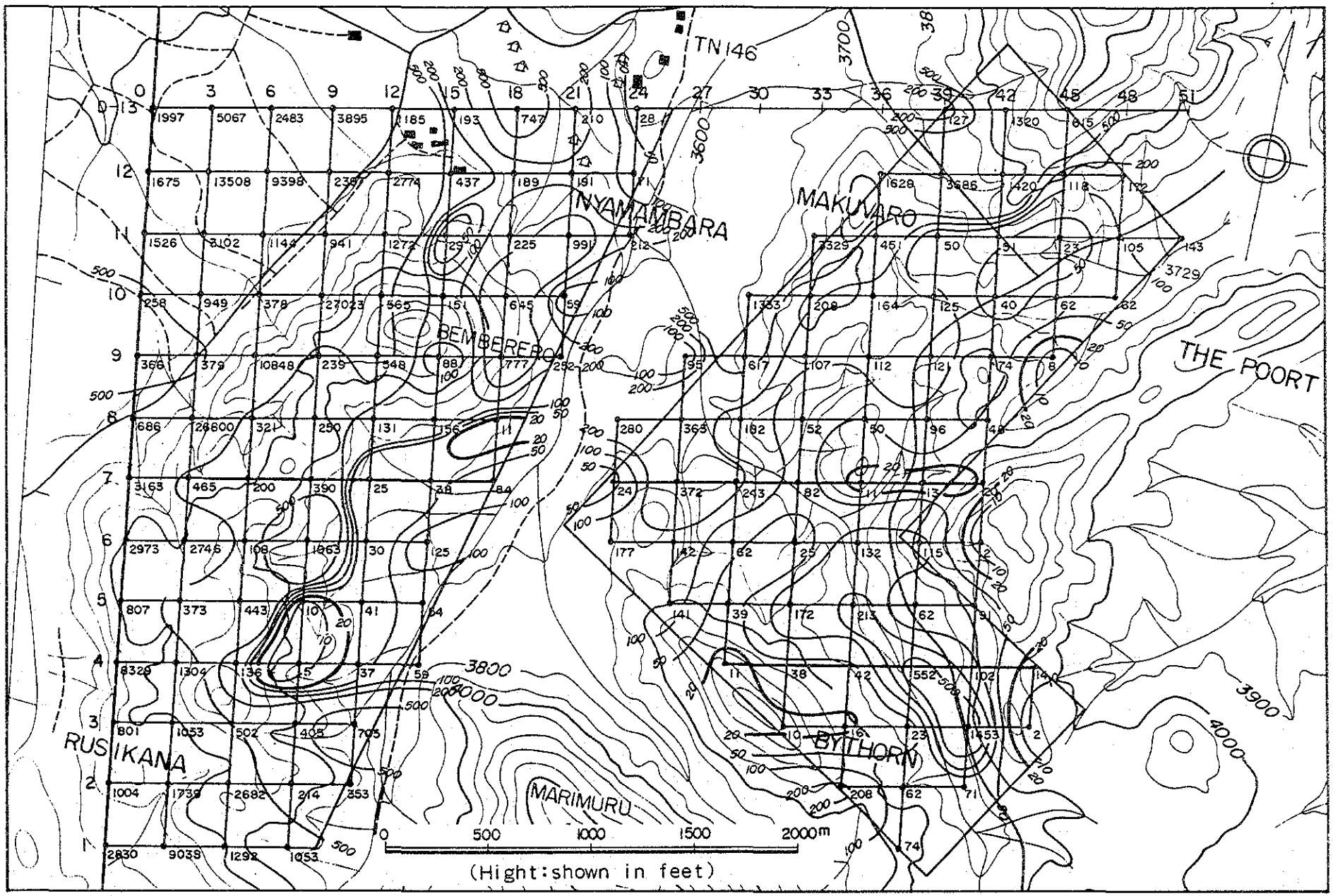

Fig. II-14 Plan of Apparent Resistivity (Area D2, D3, 256Hz) unit:Ω-m

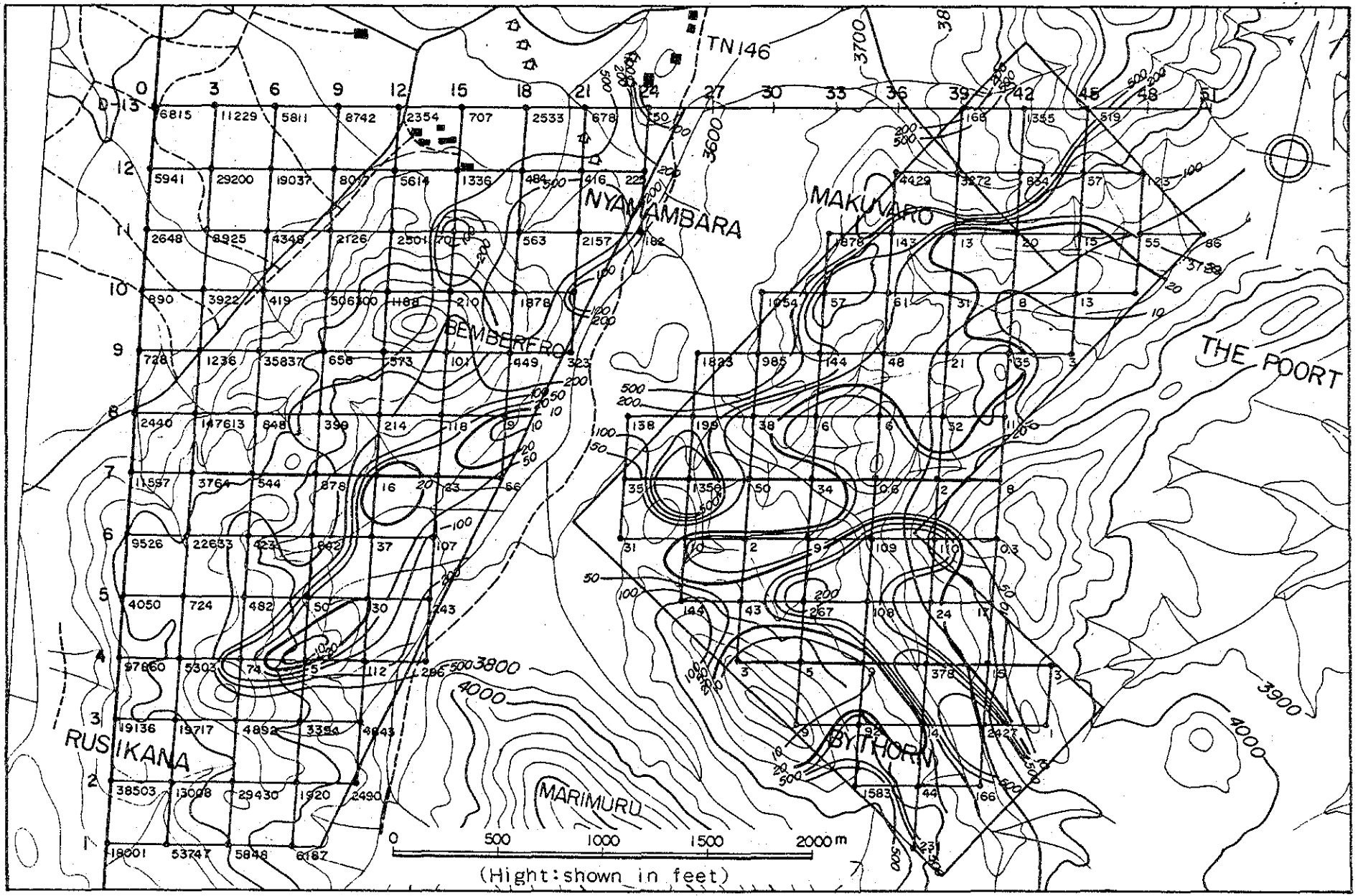

Fig. Ⅱ-15 Plan of Apparent Resistivity (Area D2, D3, 64Hz) unit:Ω-m

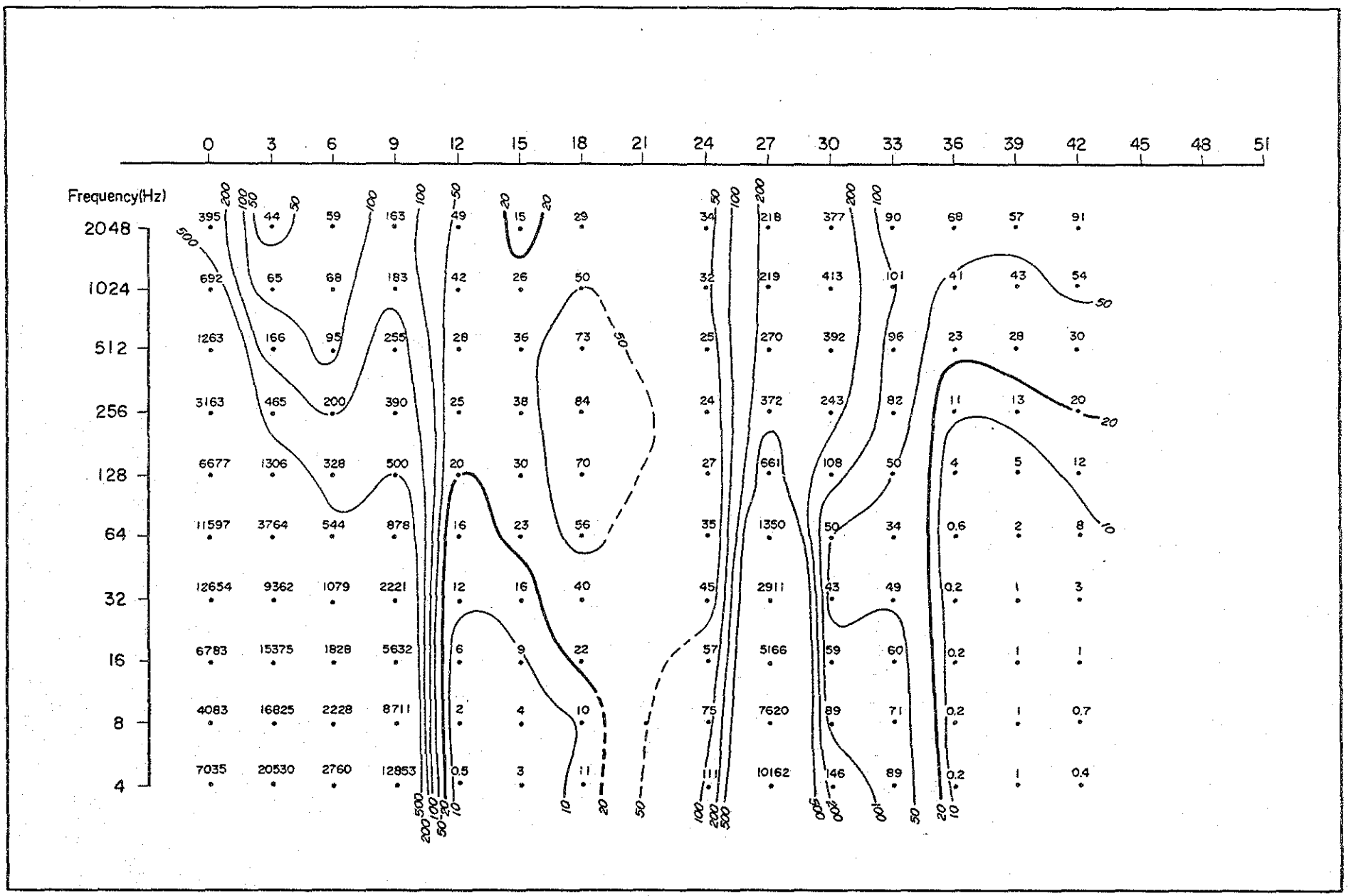

Fig. Ⅱ-16 Section of Apparent Resistivity (Line D-7) unit:Ω-m

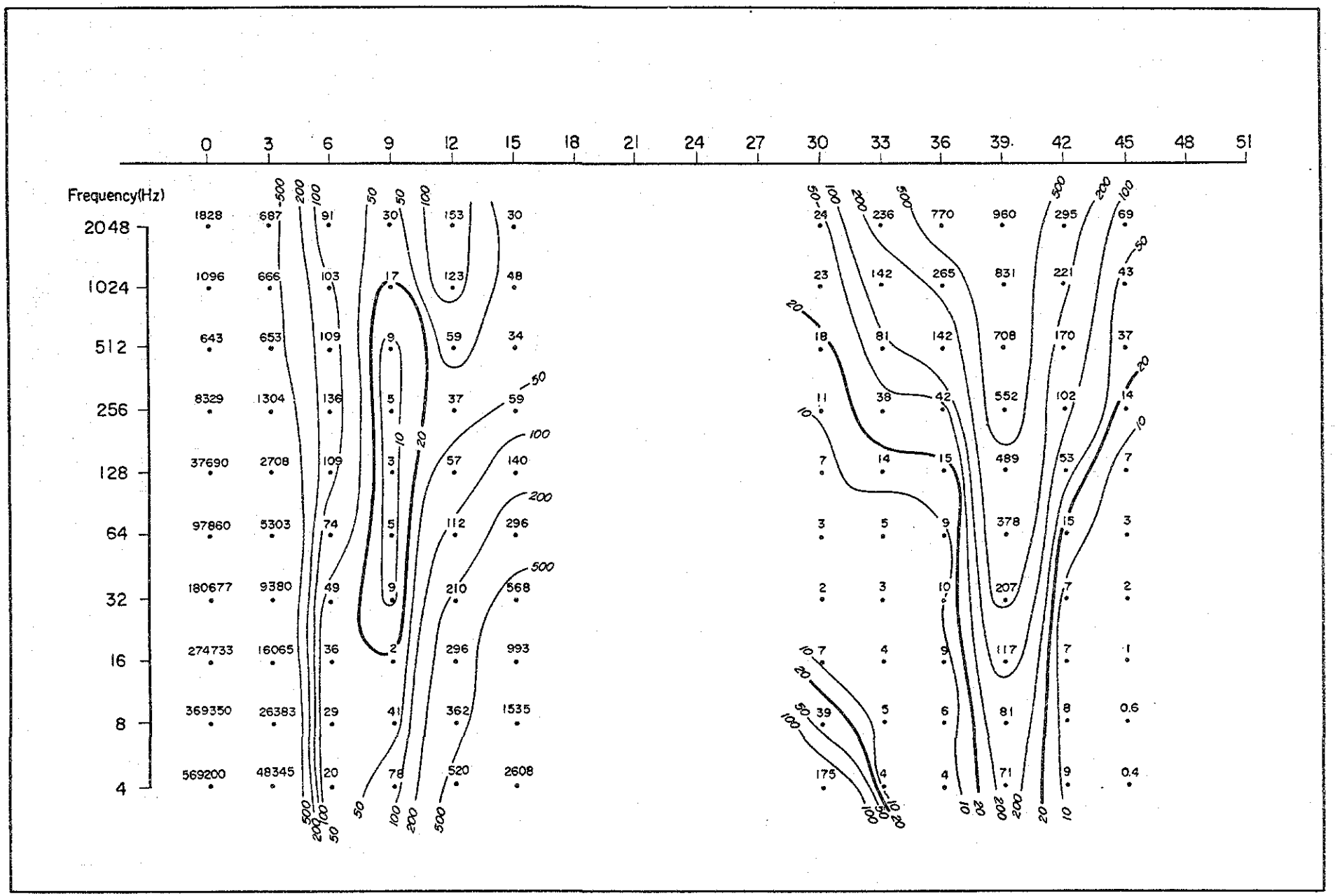

Fig. Ⅱ-17 Section of Apparent Resistivity (Line D-4) unit:Ω-m

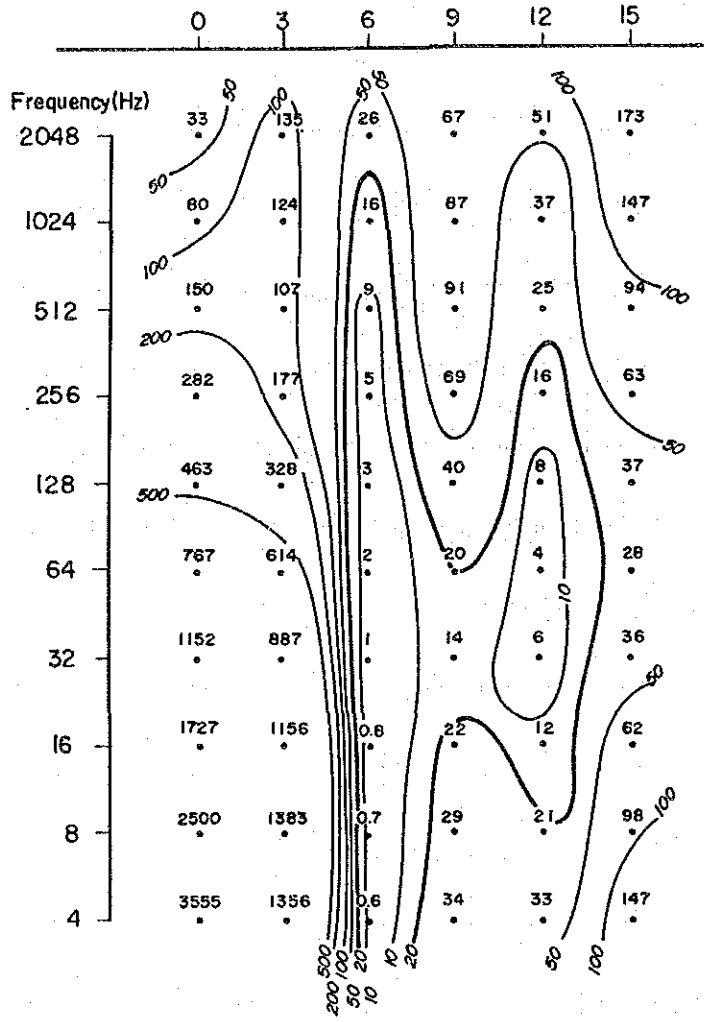

Fig. Ⅱ-18 Section of Apparent Resistivity (Line D-37) unit:Ω-m

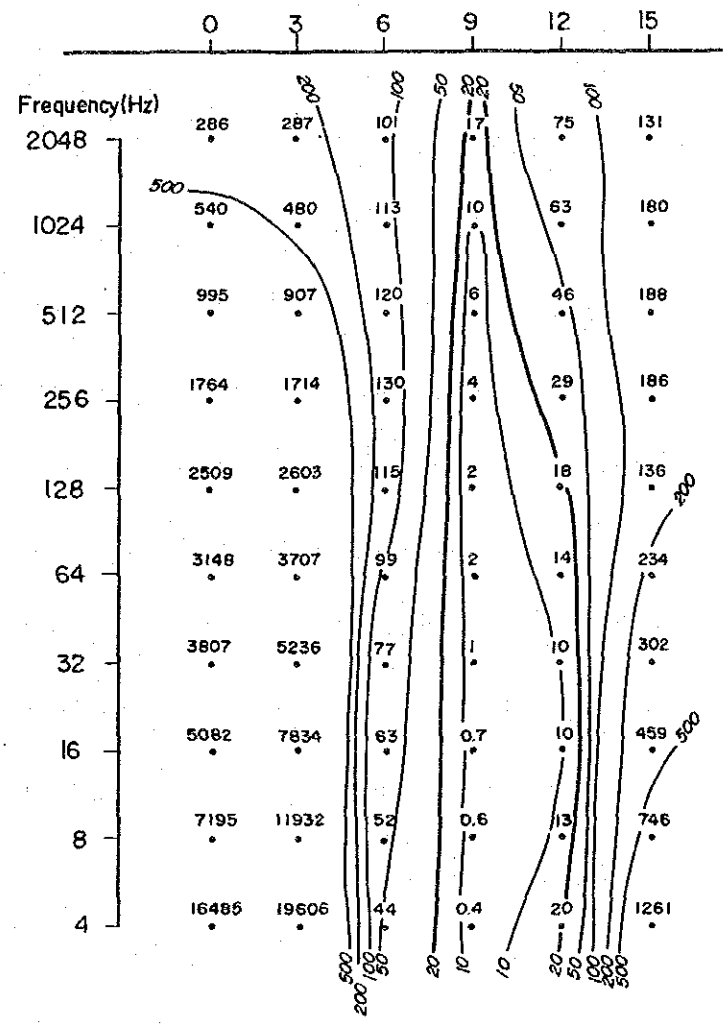

Fig. Ⅱ-19 Section of Apparent Resistivity (Line D-30) unit:Ω-m

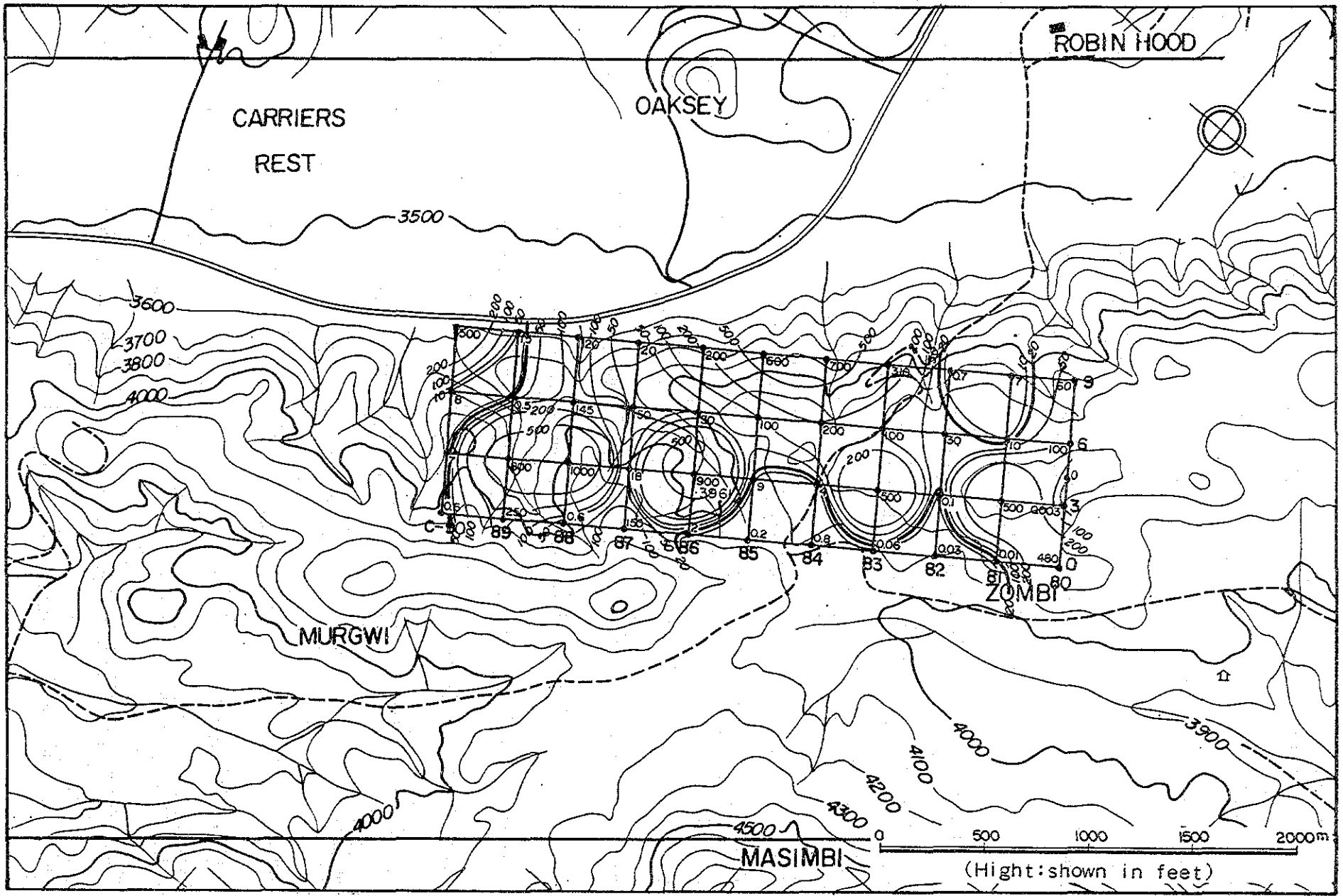

Fig. Ⅱ-20 Plan of Resistivity Structure (Area C) unit:Ω-m

A representative level, below 125m from the serface

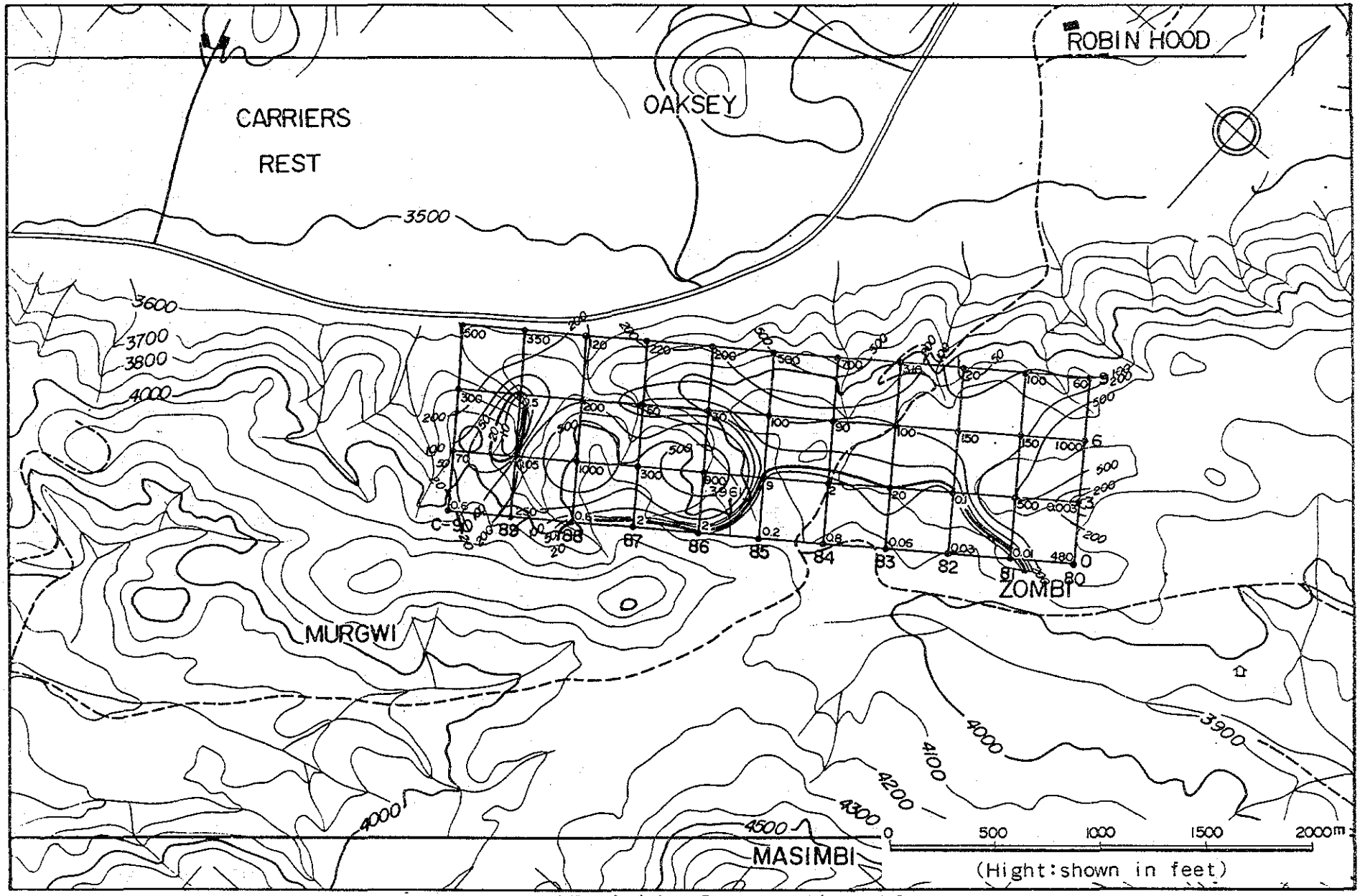

Fig. II-21 Plan of Resistivity Structure (Area C) unit:Ω-m

A representative level, below 325m from the serface

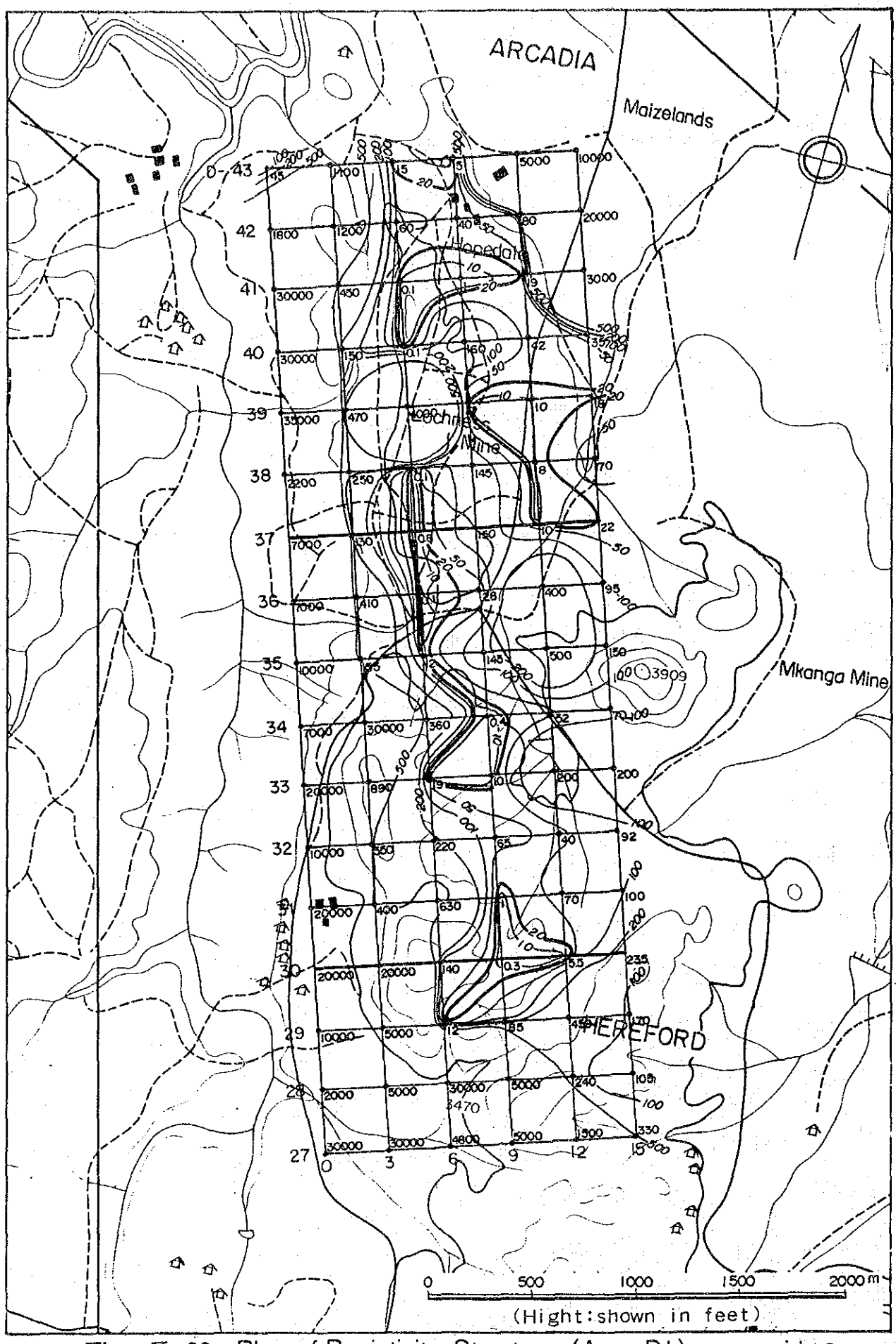

Fig. II-22 Plan of Resistivity Structure (Area D1) unit:Ω-m
A representative level, below 125m from the serface

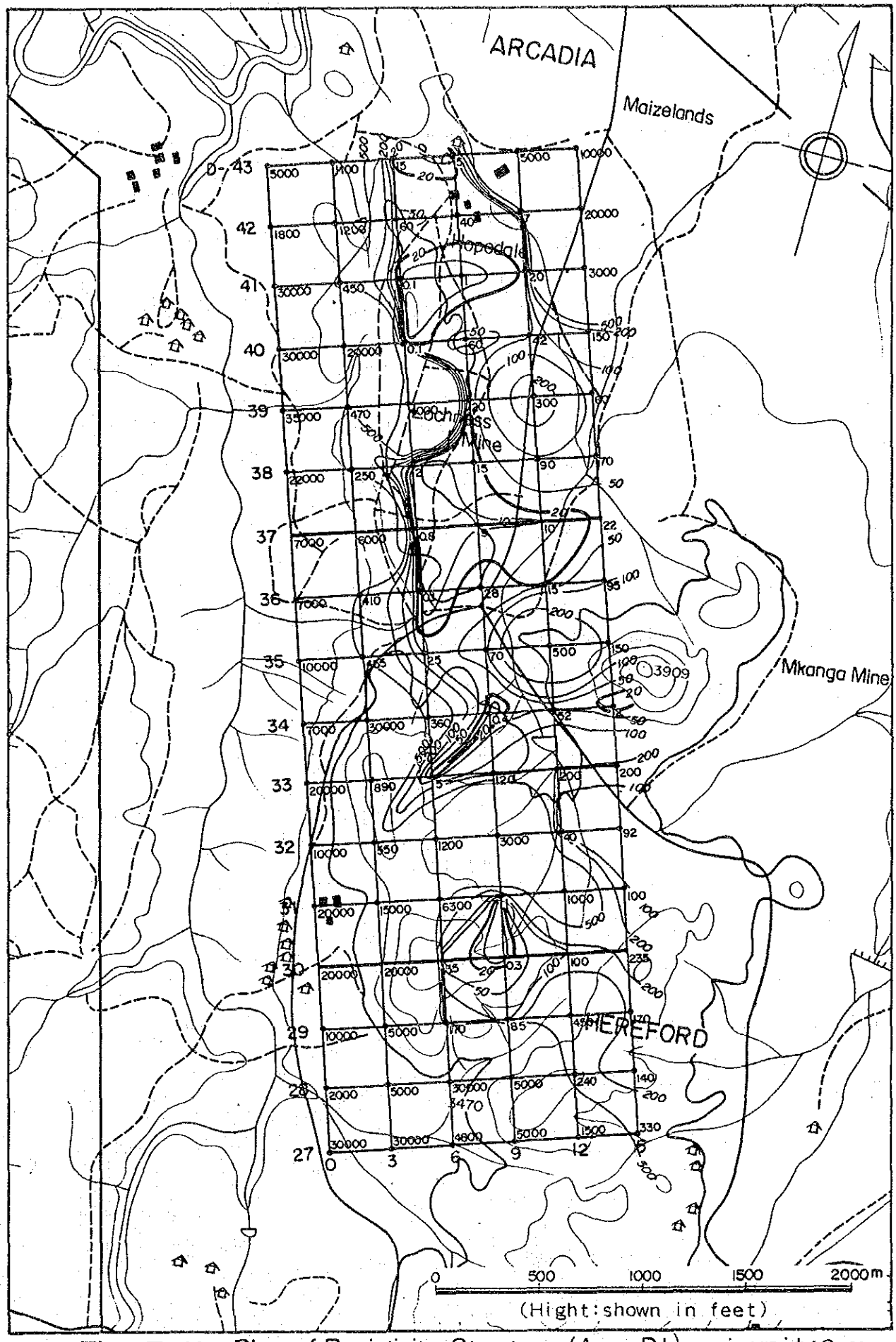

Fig. II-23 Plan of Resistivity Structure (Area DI) unit:Ω-m
A representative level, below 325m from the serface

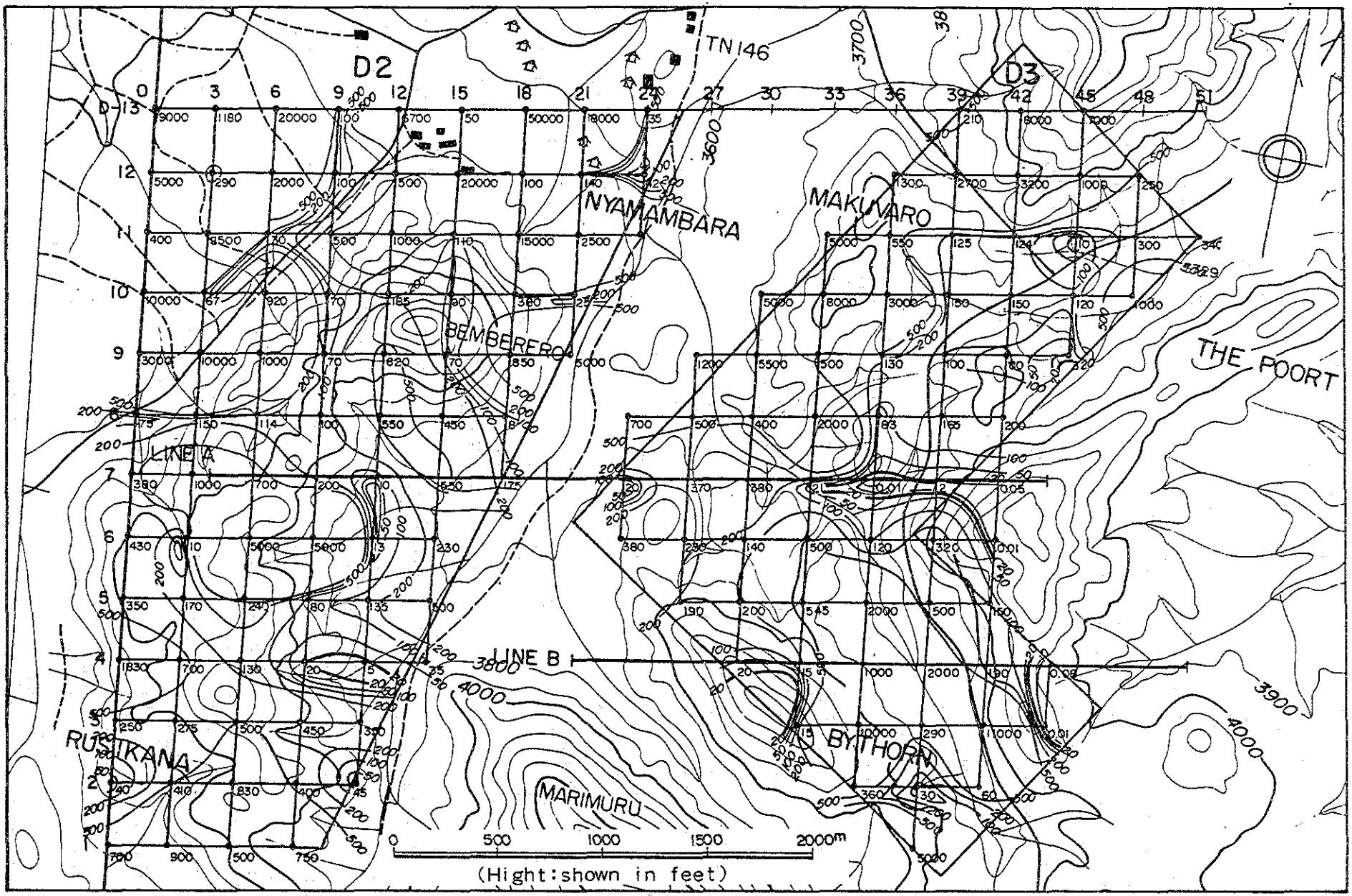

Fig. II-24 Plan of Resistivity Structure (Area D2, D3) unit:Ω-m

A representative level, below 125m from the serface

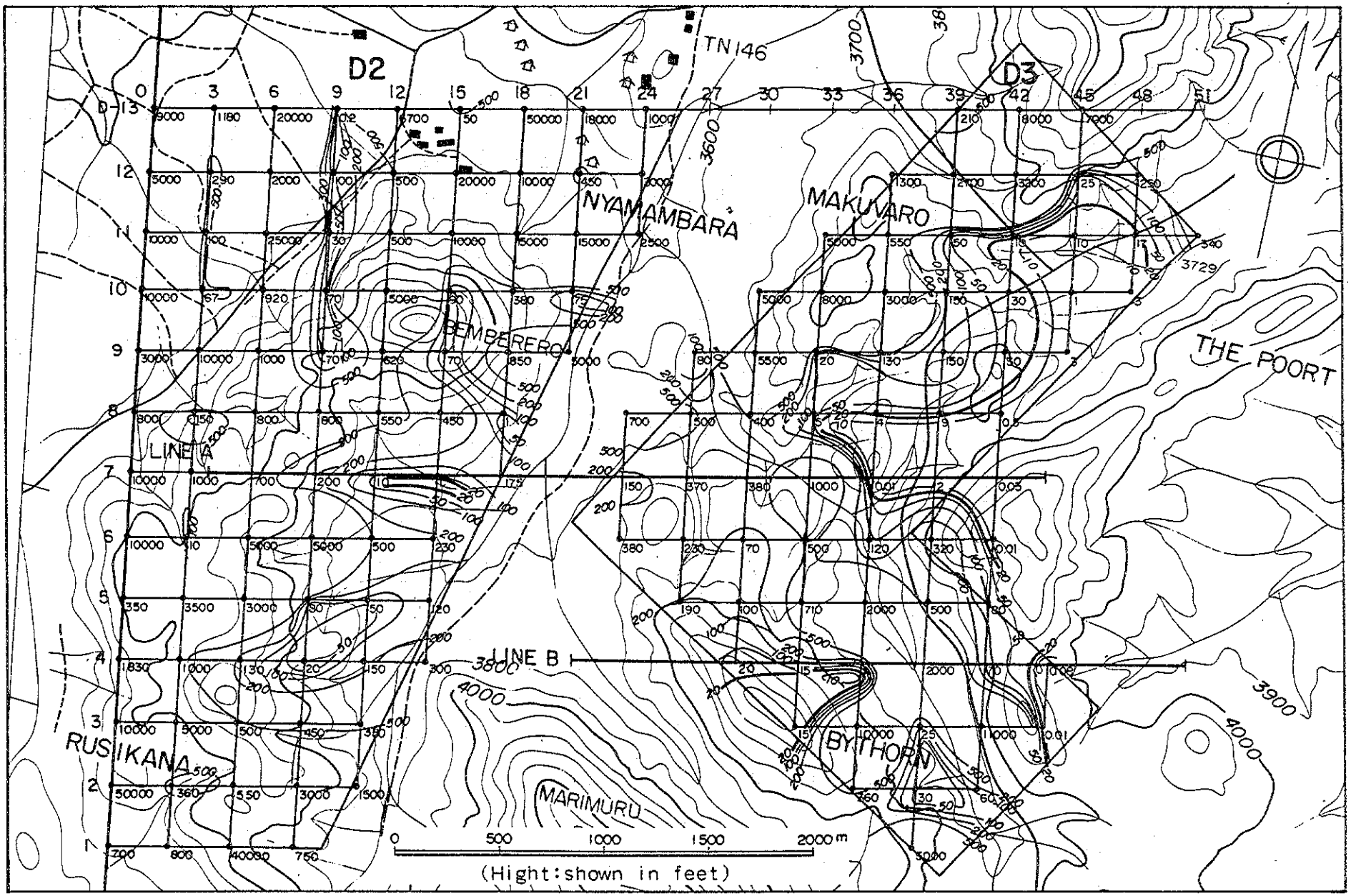

Fig. II-25 Plan of Resistivity Structure (Area D2, D3.) unit: Ω-m

A representative level, below 325m from the serface

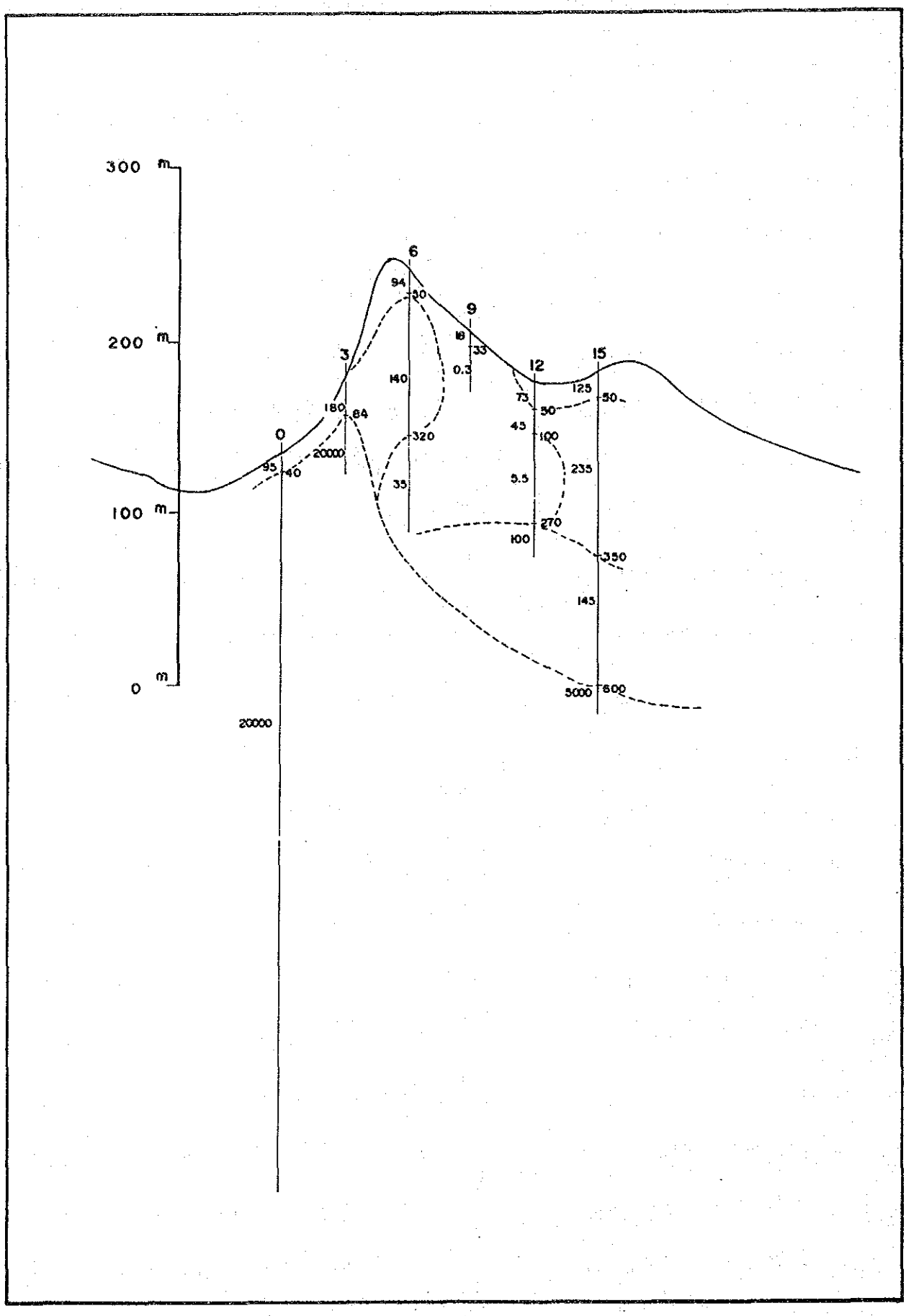

Fig. Ⅱ-26 Section of Resistivity Structure (Line D-30) unit:Ω-m

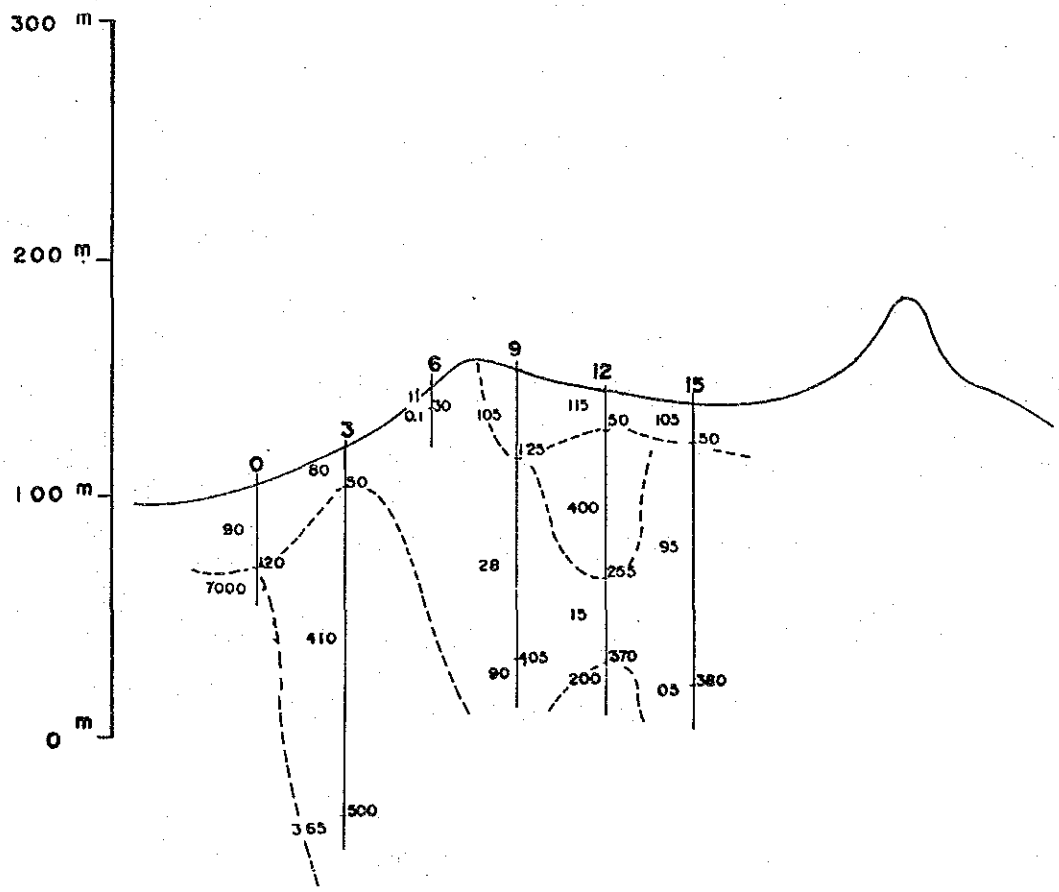

Fig. Ⅱ-27 Section of Resistivity Structure (Line D-37) unit:Ω-m

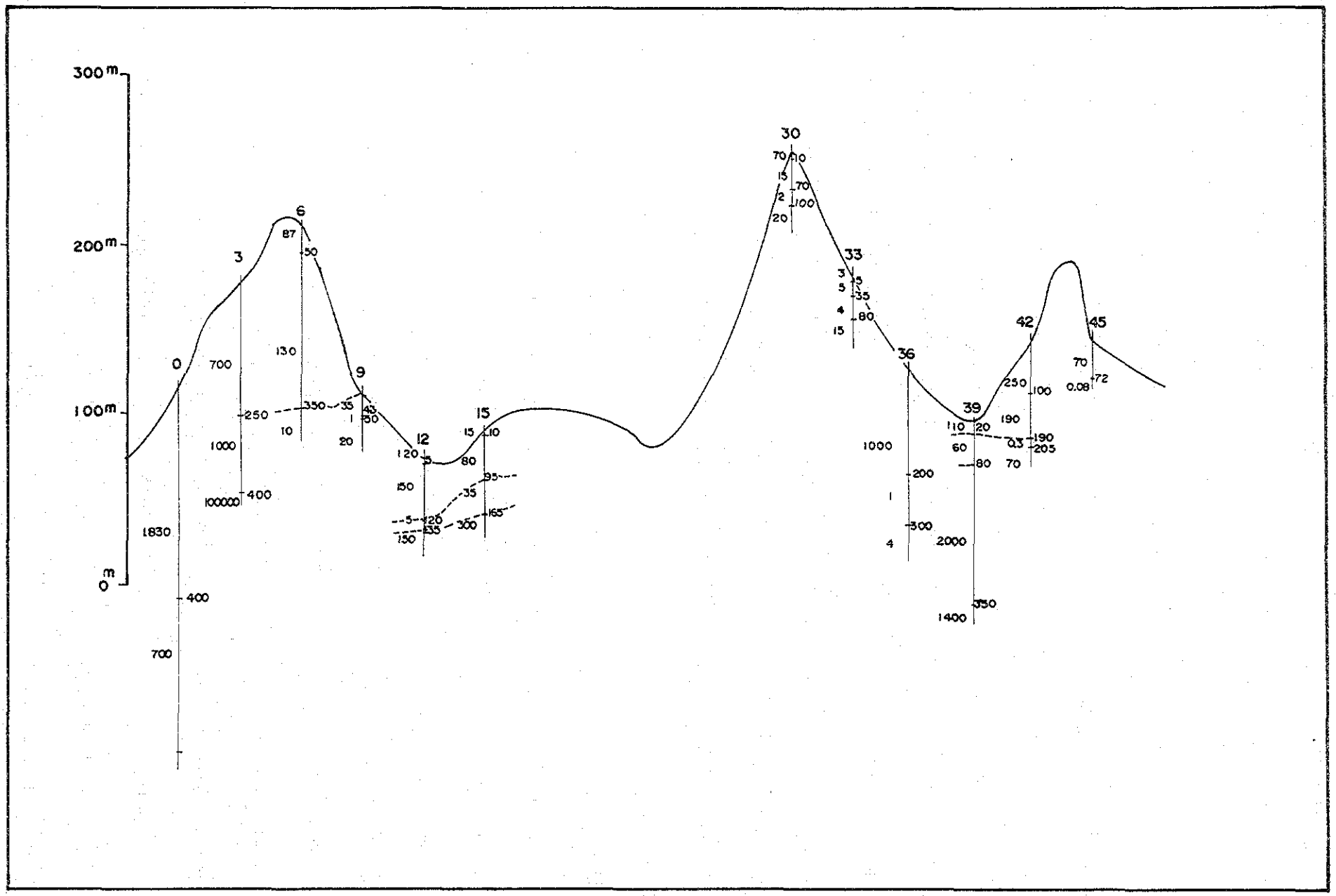

Fig. Ⅱ-28 Section of Resistivity Structure (Line D-4) unit:Ω-m

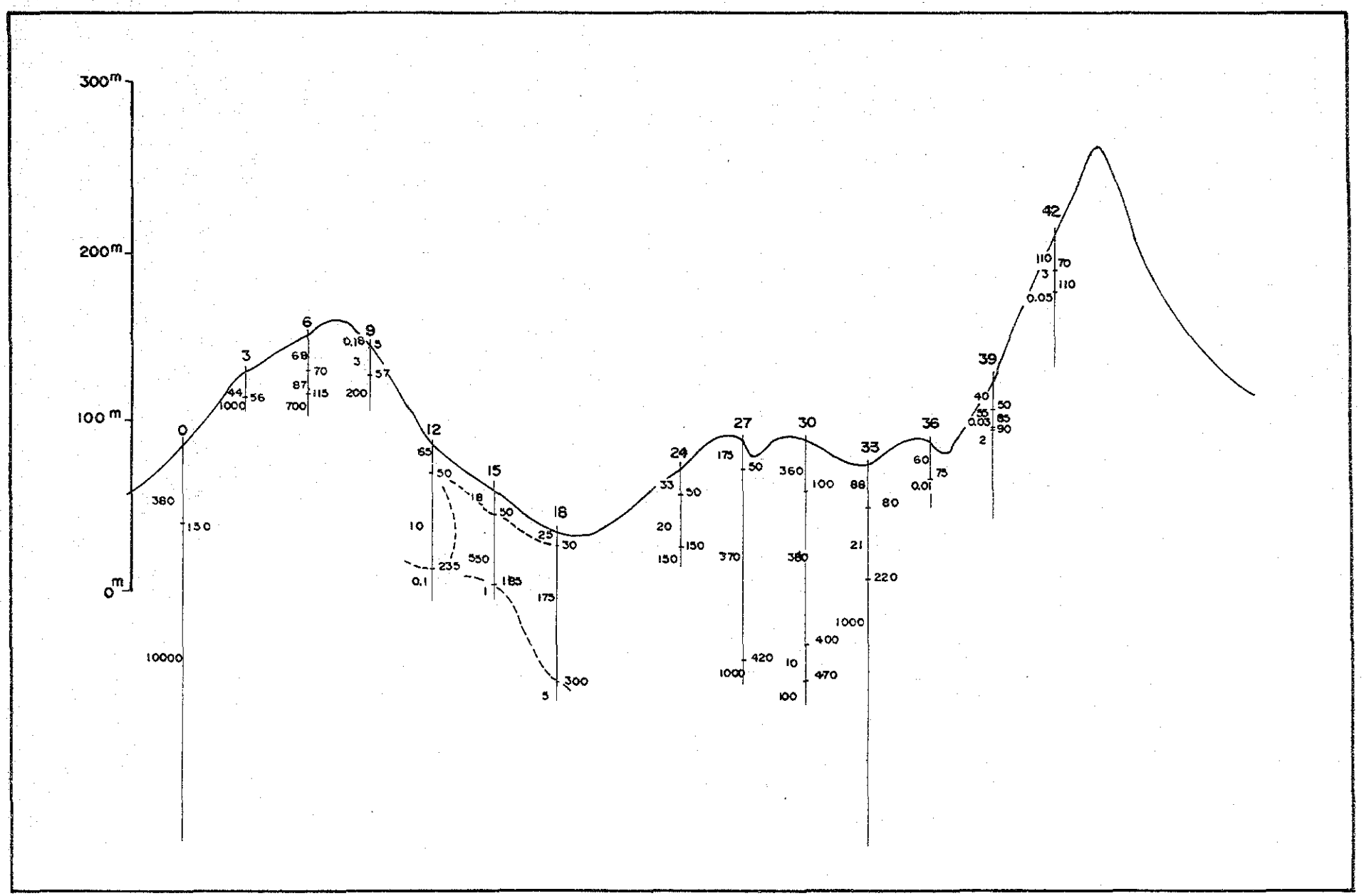

Fig. Ⅱ-29 Section of Resistivity Structure (Line D-7) unit:Ω-m

CHAPTER 3. SIP SURVEY

3-1 Survey Method

3-1-1 Measuring Method

The SIP survey method carries out measurement in a wide frequency range of 0.001 to 1,000 Hz to measure potential (Magnitude) and phase (Phase) differences and records the change of IP response as a spectrum. It is, therefore, different from frequency (IP) methods, which measure the resistivity and frequency effect due to the change of two frequencies in the range 0.1 - 5.0 Hz.

The SIP method measuring system used in this survey is shown in Fig. II-30.

Frequencies of 0.125, 1 and 8 Hz were transmitted as fundamental waves. Fourier analysis of the 3rd, 5th, 7th, 9th and 11th harmonics, received from these fundamental waves, were computed and their IP responses determined.

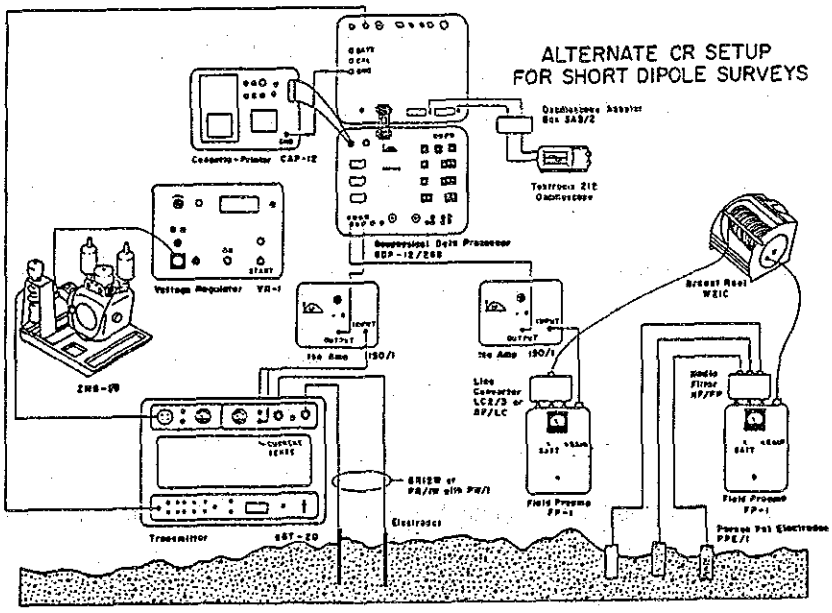

Fig. II-30 Block Diagram of Spectral IP Survey Instruments

A dipole-dipole electrode arrangement was used. Three non-polarizing electrodes, each of which consisted of a porous pot containing a copper electrode and saturated copper sulfate solution, were used as potential electrodes and were arranged as shown in Fig. II-31.

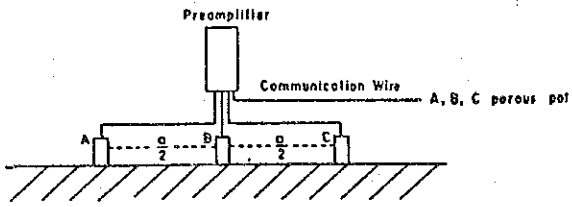

Fig. II-31 Layout of Potential Electrodes and Preamplifier

The distance (a) was 100 m and A and C were installed 50 m from the center, B. This layout was used to eliminate noise by differential amplification of the preamplifier.

Transmitted signals and received signals were synchronized to measure the magnitude and phase of many frequencies. The communication wire was stretched parallel, and 25 m apart from the main survey line, to prevent electromagnetic coupling caused by transmission currents. A plural wiring system was used for the transmission lines. 5 to 10 iron electrodes were used as the current electrodes.

3-1-2 Instruments Used

The measuring devices and instruments used for the survey are shown in Table II-5.

3-1-3 Survey Line Setting

Four SIP survey lines A (4.0 km), B (3.0 km), C (1.5 km) and D (1.5 km) were planned for the dominant, low resistivity zones found by the CSAMT method. Accordingly, new survey points were set, using pocket compasses and measuring rope, at 100 m intervals from the CSAMT survey points.

Table Ⅱ — 5 Spectral IP Survey Instruments

System	Equipment	Specification	Number
Transmitter System	Zonge Inc. Model GGT-20 Transmitter	Output Voltage: 400 ∿ 800 V Output Current: 0.2 ∿ 25 A	1
	Model ISO/1 Isolation Amplifier		2
	Model VR-1 Voltage Regulator		1
	Model 2MG-10 Engine-Generator	Max. Output Power: 10 KW Engine: 23 HP, 2 Cylinders Air-cooling	1
Receiver System	Model GDP-12 Receiver	Input Signal: 2 channels AMT Receiving Frequency: 0.5 ∿ 2048 Hz Receiving Voltage Sensitivity: 0.2 μV	1
	Model FP-12 Pre-amplifier		2
	Model CAP-12 Mini-Casset Recorder		1
	Techtronics Model 212 Oscilloscope		1
Electrode	Current Potential	Iron Rod: ϕ16 mm, 80 cm Saturated Copper Sulphate - Non-Polarized Electrode	200
Wire		VSF × 1.25 mm^2 Vinyl covered CVV_1 × .35 mm^2 Vinyl covered	1000 m 6000 m
Survey Equipment	Ushikata Pocket Compass Eslon Tape	 100 m	2 2

3-2 Data Processing and Analysis

3-2-1 Outline of SIP Method

The SIP method (usually called "Spectral IP method") is more sophisticated than the conventional IP method and it examines the change of IP effect with frequency.

In the SIP method, magnitude and phases, normalized to the lowest frequency, are measured over a wide frequency range. The results are expressed as a spectrum in relation to frequency or a Cole-Cole diagram.

Fig. II-32 shows the concept of spectral IP: (a) is the pseudosection of an ore and shows the state when ion movements are resisted or facilitated by a metallic mineral; (b) is the equivalent circuit of (a); (c) shows magnitude and phase (IP responses as a function of frequency); and (d) shows responses with time. The curves IzI and ϕ in (c) show the spectral IP responses.

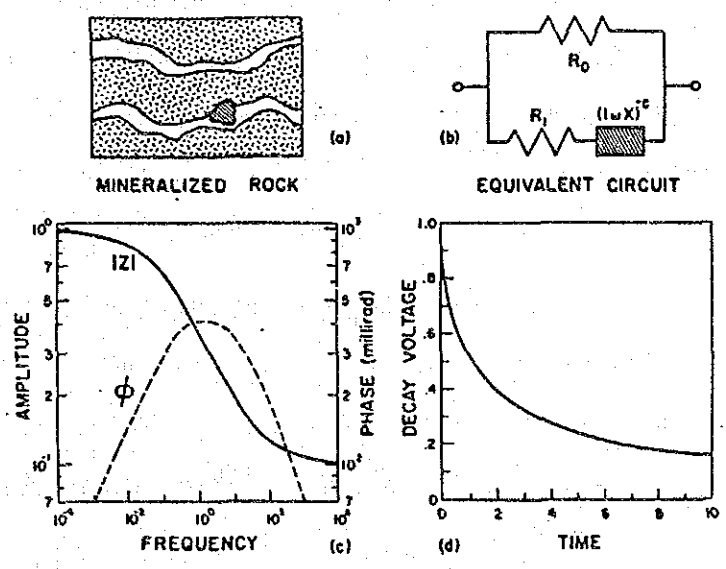

Fig. II-32 Concept of Spectral IP

Fig. II-33 illustrates concepts of "in phase" and "out of phase." When a square waveform is transmitted, a signal with a phase shift (c) and an amplitude $\overline{V}$ is received. The in-phase component has the same phase as

that of the transmitted waveform and the out-of-phase component has a 90° shifted phase as shown in the lower figures.

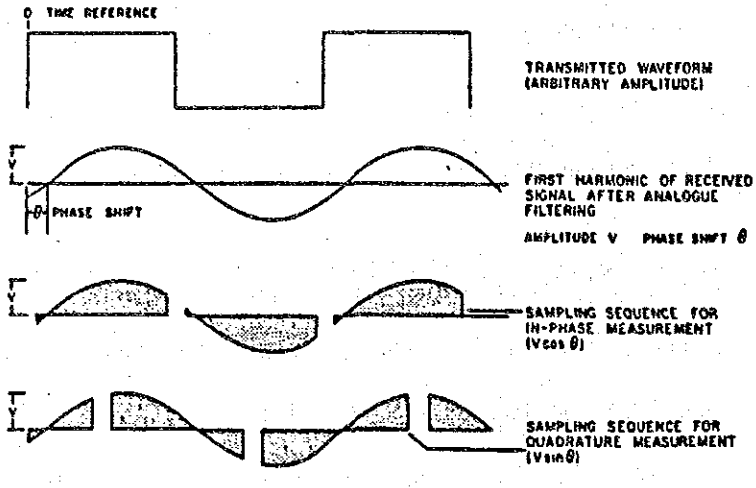

Fig. II-33 Transmitted Waveform and Received Waveform

Fig. II-34 shows the relationship between frequency and phase angle, in the form of a Cole-Cole diagram by plotting negative, out-of-phase, components on the ordinate and positive, in-phase, components on the abscissa. Intensities at 0.1 Hz and 1 Hz are M_1 and M_2 and phase angles are ϕ_1 and ϕ_2.

The frequency is almost proportional to the in-phase component and phase angle is proportional to the out-of-phase component. Chargeability also becomes a method of measuring the out-of-phase component. Black dots (.) show measured results with frequency lower to the right and higher to the left.

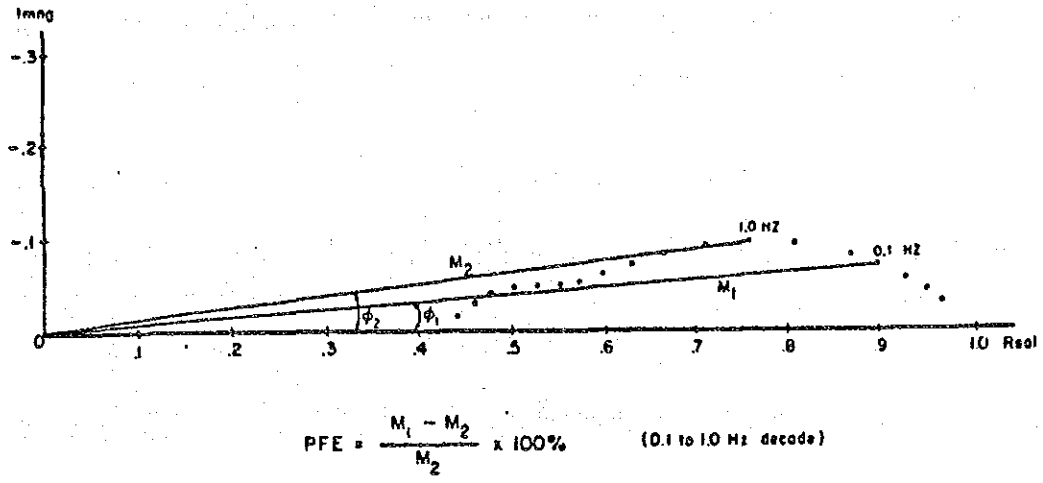

Fig. II-34 Relationship between Frequency Effect and Phase Angle

3-2-2 Data Processing

Measurement is made by transmitting fundamental waveform currents of 0.125 Hz, 1 Hz and 8 Hz. The received potential waveform, corresponding to each fundamental waveform, was processed by a GDP-12/2GB machine which carries out Fourier analyses to calculate the real and imaginary parts of each fundamental wave and its 3rd, 5th, 7th, 9th and 11th harmonics for a total of 18 frequencies. Magnitudes and phases of the 18 frequencies, resistivity of each fundamental wave, 3-point decouple phase difference and frequency effects (PEF), were printed on a cassette printer and recorded on microcassette tapes together with, transmitted current values, the errors (SEM) of the received waveforms in relation to the transmitted waveforms, the survey point numbers of current electrode couples and potential electrode separation indexes (n) and measurement conditions (gain, existence of notch filters, number of stacking times). Calibration of the measuring system was carried out everyday in the field survey, before starting operations, to correct changes in data processor circuit characteristics. Subtraction of calibration values from measured values gives pure response ground values.

Phase spectra, magnitude spectra and Cole-Cole diagrams were drawn by a computer plotter from their respective pseudosections data.

3-2-3 Results of Measuring IP Properties

The IP properties of 22 ore samples collected in the survey area were measured. Representative samples of the ores distributed in the survey area were selected, including the same ores with different degrees of alteration, to provide as many types of samples as possible. Samples were collected evenly from all the D-3, D-2, D-1 and C areas.

A diagram representing the measuring method is shown in Fig. II-35 and measured results are shown in Table II-6.

The phase difference spectra, magnitude spectra, and Cole-Cole figures are shown in Fig. II-36.

The ores show low resistivity and high IP effect. Serpertines, tuffs, and banded ironstones show relatively low resistivity, but moderate IP effect.

The phase difference of the ore is very high (about 800 m rad peak) but the resistivity ranges from 59 Ω-m at 0.125 Hz to 45 Ω-m or 88 Hz.

These properties of the ore sample are clearly different from, those of other rocks.

3-2-4 Analytical Methods

Analyses for SIP anomalies were carried out by preparing the following plans, sections and spectrum figures from the measured data, outlined below:

(1) Apparent resistivity plans and sectional views (0.125 Hz)

(2) PFE plans and sectional views (0.125 Hz)

These were displayed similarly to IP data on pseudosections and normal analytical methods were applied.

(3) Phase sectional views (each frequency)

obtained directly from the printed results and displayed on pseudo-sections.

(4) Magnitude spectrum diagrams

The diagrams show change of potential proportional to apparent resistivity. Resistivity data are normalized with the potential of the lowest frequency (0.125 Hz). Frequencies are plotted on the abscissa, and the normalized data on the ordinate, using bi-logarithmic scale paper.

(5) Phase spectrum diagrams

The diagrams show phase difference data between the transmitter and the receiver for each frequency. Frequencies are plotted on the abscissa and phase differences on the ordinate, using bi-logarithmic scale paper.

(6) Cole-Cole diagrams

The diagrams express magnitude and phase data corresponding to the change of frequency obtained by the measurement on one plane (complex plane). They have the advantage of showing the data in (4) and (5) simultaneously.

Real components are plotted on the abscissa and imaginary components on the ordinate. If the magnitude and phase for each frequency are M and ϕ respectively, then components can be determined from the following equations (Table II-7).

Re (real component) = M cos ϕ

Im (imaginary component) = M sin ϕ

(7) 3-point decouple phase difference diagrams

These phase differences are those of an approximate direct current, calculated utilizing phase differences between 0.125 Hz, 0.375 Hz and 0.625 Hz. It is assumed that a quadratic functional

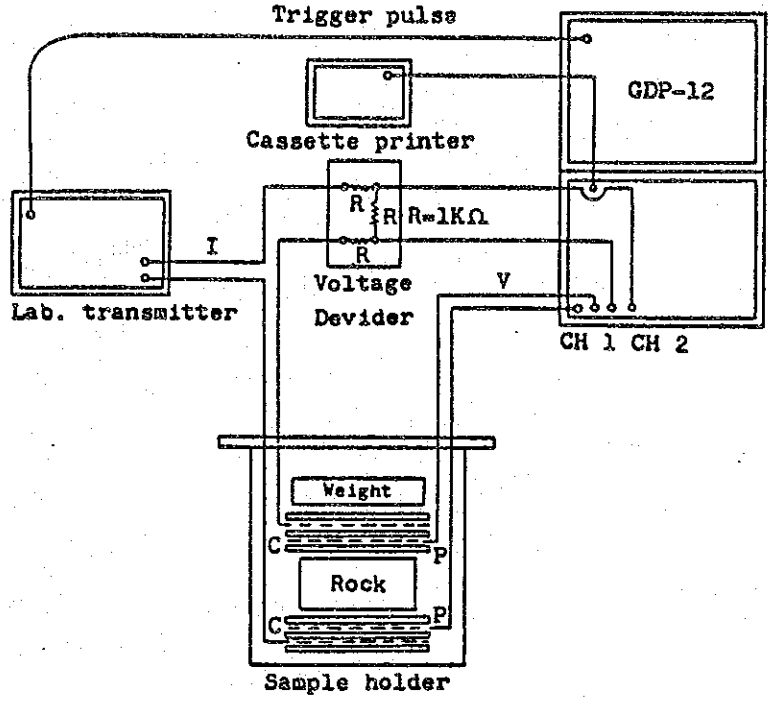

Fig. Ⅱ - 3 5 Block Diagam of Laboratory Measurement

Table II-6 IP Propaties of Ore and Rock Sample

No.	Sample No.	Resistivity 0.125Hz(Ω-m)	Raw Phase 0.125Hz(-mrad)	3ptDecoupled (-mrad)	P.F.E. (%)	Rock name	Sample Locality
1	1	792	3.08	-0.43	1.04	Banded Ironstone, cherty part	D-3
2	2	1111	15.0	15.7	1.84	Banded Ironstone, iron-rich part	D-3
3	3	1531	11.1	10.5	1.54	Banded Ironstone, hard cherty part	D-3
4	5	3028	11.0	11.1	1.45	Serpentinite, strong	D-3
5	9	1214	6.95	4.48	1.35	Serpentinite, weak	D-3
6	10	17011	14.0	12.70	2.07	Pyroxene Andesite,(komatiite ?)	D-3
7	12	2768	7.53	6.79	1.14	Dolerite	D-3
8	13	2571	11.33	9.02	1.91	Chert,(sandstone ?)	D-3
9	14	2078	10.1	9.73	1.43	Granite	D-3
10	15	8989	10.1	8.95	1.59	Gabbro	D-3
11	16	4072	5.13	4.37	0.86	Andesite	D-3
12	18	1707	9.52	8.78	1.39	Andesite, weak serpentinized	D-2
13	19	3671	3.74	3.66	0.61	Pegmatitic Granite	D-2
14	20	611	13.35	16.0	1.25	Serpentinite	D-1
15	27	498	5.77	2.91	1.34	Acidic tuff	D-1
16	28	173	3.11	-3.01	1.58	Serpentinite	D-1
17	21	9864	3.70	3.12	0.61	Basalt	C
18	22	8691	7.13	5.75	1.06	Dolerite	C
19	23	8642	5.68	5.14	0.84	Porphyrite	C
20	24	21760	4.30	3.74	0.66	Basalt, weak serpentinized	C
21	30	14040	4.41	4.40	0.63	Komatiite	C
22	31	59	54.01	457.7	138.4	Ni-Cu Ore	Trojan

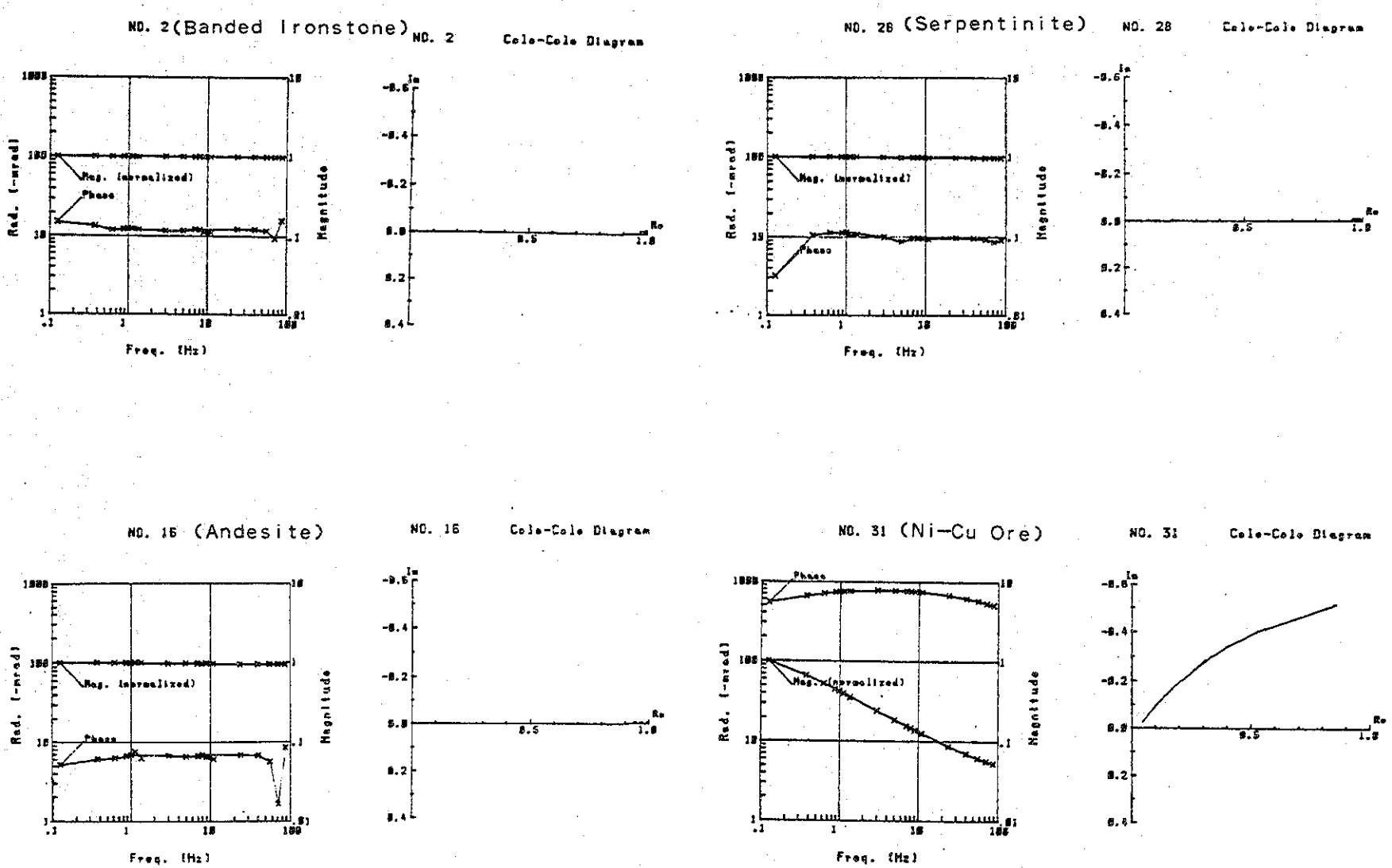

Fig. Ⅱ-36 Phase Spectral of Rocks Samples

Table II-7 Calculation of Real Part, Imaginery Part

Hz	Rate of Magnitude	Normalize	Phase difference	Real	Imaginery
0.125	$M_1/M_2=M_4$	$M_4/M_4=N$ (=1)	ϕ_4	$N_4\cos\phi_4$	$N_4\sin\phi_4$
0.375	" $=M_5$	$M_5/M_4=N$	ϕ_5	$N_5\cos\phi_5$	$N_5\sin\phi_5$
0.625	" $=M_6$	$M_6/M_4=N$	ϕ_6	$N_6\cos\phi_6$	$N_6\sin\phi_6$
0.875	" $=M_7$	$M_7/M_4=N$	ϕ_7	$N_7\cos\phi_7$	$N_7\sin\phi_7$
1	" $=M_8$	$M_8/M_4=N$	ϕ_8	$N_8\cos\phi_8$	$N_8\sin\phi_8$
1.125	" $=M_9$	$M_9/M_4=N$	ϕ_9	$N_9\cos\phi_9$	$N_9\sin\phi_9$
1.375	" $=M_{10}$	$M_{10}/M_4=N$	ϕ_{10}	$N_{10}\cos\phi_{10}$	$N_{10}\sin\phi_{10}$
3	" $=M_{11}$	$M_{11}/M_4=N$	ϕ_{11}	$N_{11}\cos\phi_{11}$	$N_{11}\sin\phi_{11}$
5	" $=M_{12}$	$M_{12}/M_4=N$	ϕ_{12}	$N_{12}\cos\phi_{12}$	$N_{12}\sin\phi_{12}$
7	" $=M_{13}$	$M_{13}/M_4=N$	ϕ_{13}	$N_{13}\cos\phi_{13}$	$N_{13}\sin\phi_{13}$
8	" $=M_{14}$	$M_{14}/M_4=N$	ϕ_{14}	$N_{14}\cos\phi_{14}$	$N_{14}\sin\phi_{14}$
9	" $=M_{15}$	$M_{15}/M_4=N$	ϕ_{15}	$N_{15}\cos\phi_{15}$	$N_{15}\sin\phi_{15}$
11	" $=M_{16}$	$M_{16}/M_4=N$	ϕ_{16}	$N_{16}\cos\phi_{16}$	$N_{16}\sin\phi_{16}$
24	" $=M_{17}$	$M_{17}/M_4=N$	ϕ_{17}	$N_{17}\cos\phi_{17}$	$N_{17}\sin\phi_{17}$
40	" $=M_{18}$	$M_{18}/M_4=N$	ϕ_{18}	$N_{18}\cos\phi_{18}$	$N_{18}\sin\phi_{18}$
56	" $=M_{19}$	$M_{19}/M_4=N$	ϕ_{19}	$N_{19}\cos\phi_{19}$	$N_{19}\sin\phi_{19}$
72	" $=M_{20}$	$M_{20}/M_4=N$	ϕ_{20}	$N_{20}\cos\phi_{20}$	$N_{20}\sin\phi_{20}$
88	" $=M_{21}$	$M_{21}/M_4=N$	ϕ_{21}	$N_{21}\cos\phi_{21}$	$N_{21}\sin\phi_{21}$

relationship ($\phi = a.f^2 + b.f + c$) exists between frequecies (f) and phase differences (ϕ). In the equation, c is the phase difference at a frequency very close to direct current, i.e., 3-point decouple phase difference.

If the phase differences at 0.125 Hz, 0.375 Hz and 0.625 Hz are expressed as $\phi 0.125$, $\phi 0.375$ and $\phi 0.625$, then c is given by the following equation.

$$c = \frac{15}{8}\phi 0.125 - \frac{10}{8}\phi 0.375 + \frac{3}{8}\phi 0.625$$

3-3 Survey Result and Discussion

3-3-1 Survey Results

General tendencies (apparent resistivity, PFE, phase differences, etc.) for survey lines A to D, based on the results obtained from the above analysis, and the anomalous zones found in this survey are described in the discussion section.

(1) Survey Line A

The apparent resistivity of this survey line suggests the existence of low resistivity zones below (10 Ω-m) under survey points 8 to 10 (n = 2 - 5), under survey point 31 and eastward (n = 2 - 5). Under survey points 34 to 37, a very low resistivity value of about 1 Ωm was found.

From survey point 9 westward, under survey points 11 to 20 (n = 2 - 5) and under survey points 23 to 29 (n = 1 - 5), high resistivity zones (above 100 Ω-m) are thought to exist.

High PFE values of 5% or more were noticed at the low resistivity zones of the above-mentioned three places. Additionally, a negative coupling phenomenon was observed from the spectral characteristics of phase difference which seems to reflect the contrasting high resis-

tivity underground structure. This anomalous zone is discussed later as the first priority anomalous zone. Negative coupling for 3 point decouple phase differences was predominant, and decoupling by this technique is thought to be difficult, so it was omitted from this report. Low PFE values (2% or less) were noticed at the high resistivity zones mentioned above and the spectum characteristics of phase differences are shown by a straight line with a gradient of almost 45° with frequency increase. This is the usual electromagnetic coupling phenomenon, occurring when IP effects scarcely exist.

In the eastward inclined zone, under survey point 23.5 (n = 3), and the westward inclined zone, under survey point 29.5 (n = 1), spectrum characteristics in the several Hz or less frequency band, show a tendency to constancy or slightly rightward-decrease with frequency increase. This anomalous zone is discussed as the second priority anomalous zone later (Figs. II-35-1∿1, Figs. II-39-1∿2).

(2) Survey Line B

The apparent resistivity of this survey line shows low values (n = 3-5) over its whole length and suggests the existence of low resistivity zones (below 10 Ω-m) especially under survey points 30 to 32 (n = 1 - 5), under survey points 35 to 38 and under survey point 42 eastward (n = 3 - 5).

High PFE values (5% or more) were found at the low resistivity zones of the above-mentioned, three places.

The spectrum characteristics of phase difference show a tendency to constancy, or slightly rightward-decrease, with frequency increase at survey point 32 and westward (n = 1 - 2), under survey points 39 to 41 (n = 1 - 3) and at survey point 44 and eastward (n = 1 - 2). A negative coupling phenomenon was observed over almost the entire

area except at the above three places. The former anomalous zone is graded as the second priority anomalous zone and the latter, the first priority anomalous zone. Both are discussed later (Fig.s II-36-1∿3, Fig.s II-40-1∿2).

(3) Survey Line C

The apparent resistivity of this survey line suggests the existence of low resistivity zones (below 10 Ω-m) under survey points 4 to 7 (n = 2 - 5).

High resistivity zones (above 100 Ω-m) are supposed to exist west of survey point 5 (n = 1 - 3) and east of survey point 7 (n = 1 - 3). High PFE values (above 5%) were noticed at the low resistivity zones mentioned above and their spectral phase difference characteristics show negative coupling phenomena. This anomalous zone is discussed later as the first priority anomalous zone.

Spectral characteristics of phase difference at the above-mentioned high resistivity zones, show a gradient of almost 45° with frequency increase, which represents normal electromagnetic coupling phenomenon, when IP effects scarcely exist. Phase difference spectrum characteristics in the low frequency band, at the eastward inclined zone under survey point 6.5 (n = 1 - 4), show a tendency to constancy, or slightly rightward decrease, with frequency increase. This anomalous zone is discussed later as the second priority anomalous zone (Figs. II-37-1∿3, Figs. II-41-1∿2).

(4) Survey Line D

The apparent resistivity of this survey line suggests the existence of low resistivity zones (below 10 Ω-m) under survey points 7 to 10 (n = 1 - 2) and shows very low resistivity values (below 1 Ω-m) especially at n = 2 - 3.

High PFE values (above 10%) were noticed at the above-mentioned low resistivity zones. Negative coupling phenomena were noticed from the phase difference spectrum characteristics. This anomalous zone is discussed later as the first priority anomalous zone.

West of survey point 6 (n = 1 - 2) and east of survey point 11 (n = 1 - 2), high resistivity zones (above 100 Ω-m) are thought to exist. Phase difference spectrum characteristics show normal electromagnetic coupling phenomenon, occurring when IP effects scarcely exist.

The phase difference spectrum characteristics in the low frequency band at the eastward inclined zone under survey point 10.5 (n = 1 - 3), show a tendency to constancy, or slightly rightward-decrease, with frequency increase. This anomalous Zone is discussed later as the second priority anomalous zone (Figs. II-38-1∿3, Figs. II-42-1∿2).

3-3-2 Discussion

Two anomalous zones (A and B) with strong IP effect were found by the SIP method survey this year.

Features of each anomalous zone are described as follows:

(1) First Priority Anomalous Zone

The negative coupling phenomenon is predominant in this anomalous zone, which usually reflects non-uniformity of resistivity structure. It is a phenomenon which particularly appears when a low resistivity zone exists locally in a high resistivity zone, which agrees with the area survey results.

East of survey point 31 on survey line A, the negative coupling phenomenon is noticed over a wide range, and under survey point 21.5 a ( )-shaped characteristic is found.

On survey line B, negative coupling is found over almost the

entire region, except parts west of survey point 32 (n = 1 - 2), under survey points 39 to 41 (n = 1 - 3) and east of survey point 44 (n = 1 - 2).

The above-mentioned anomalous zones found on survey lines A and B are thought to be caused by the same rocks of very high conductivity because of the similarity of spectral characteristics.

Negative coupling is noticed under survey point 5.5 (n = 1 - 5) on survey line C and under survey point 8 (n = 1 - 5) on survey line D. The negative coupling is thought to result from the same rocks of very high conductivity because the ( )-shaped characteristic is found in both places and their spectral characteristics are similar.

(2) Second Priority Anomalous Zone

This anomalous zone is characterized by a tendency to constancy, or slight rightward-falling phase difference spectrum characteristics, with frequency increase, in the frequency band below several Hz. Spectrum characteristics like this usually have high IP effects. On survey line A, this second priority anomalous zone is noticed in the eastward inclined zone under survey point 23.5 (n = 3) and in the westward inclined zone under survey point 29.5 (n = 1). On survey line B, it is noticed west of survey point 32 (n = 1 - 2), under survey points 39 to 41 (n = 1 - 3) and east of survey point 44 (n = 1 - 2).

Both the above anomalous zones are situated on the periphery of the first priority anomalous zone, and are thought to result from rocks which are changing to the first priority anomalous zone's types.

Also, on survey lines C and D, this second priority anomalous zone is noticed on the periphery of anomalous zone A detected on each survey line.

Geological set-up relating to these anomalous zones and their

apparent resistivity values are described below:

Survey line A

The apparent resistivity distribution shows notable low resistivity zones (below 10 Ω-m) under survey points 8 to 10, 21 to 22 and under survey point 31 and eastward.

Low resistivity under survey points 8 to 10 agrees with the distribution of serpentinite and banded ironstone.

There is a possibility of mineralized zones in this area because the Trojan ore deposit is situated on the boundary of the two layers. The part under survey points 31 to 42 is associated with banded ironstone.

Survey line B

Low resistivity zones (below 10 Ω-m) are found under survey point 30 to 32, 35 to 38 and under survey point 42 and eastward. Low resistivity under survey points 3 to 32 and the part under survey points 35 to 38 is associated with banded ironstone. The part under the east of survey point 42 agrees with the banded ironstone - sedimentary rock boundary.

Survey line C

The apparent resistivity distribution shows a notable low resistivity zone (below 10 Ω-m) under survey points 4 to 7. Mineralized zones in serpentinite or mineralized zones caused by the intrusion of pegmatite are suspected.

Survey line D

The apparent resistivity distribution shows a notable low resistivity zone (below 10 Ω-m) under survey points 7 to 10. Mineralized zones in serpentinite or mineralized zones caused by the intrusion of pegmatite are suspected.

(Reference Data)

A SIP test survey was conducted on the Trojan deposits to get reference data. The test result of the survey on the survey line "A" is shown in Fig. II-37, 38.

From the spectral charactors of the phase difference, negative coupling phenomena reflecting geological stractures which have clear resistivity contrast, were detected. This kind anomaly was named as First Class Anomaly as mentioned in Chapter 3, 3-3-1. These anomalies found in the test area are supposed to be caused by very conductive rocks, and shows the effect of the Trojan deposits.

The test result gave us a good guide line for analysis of the SIP survey results in the survey areas.

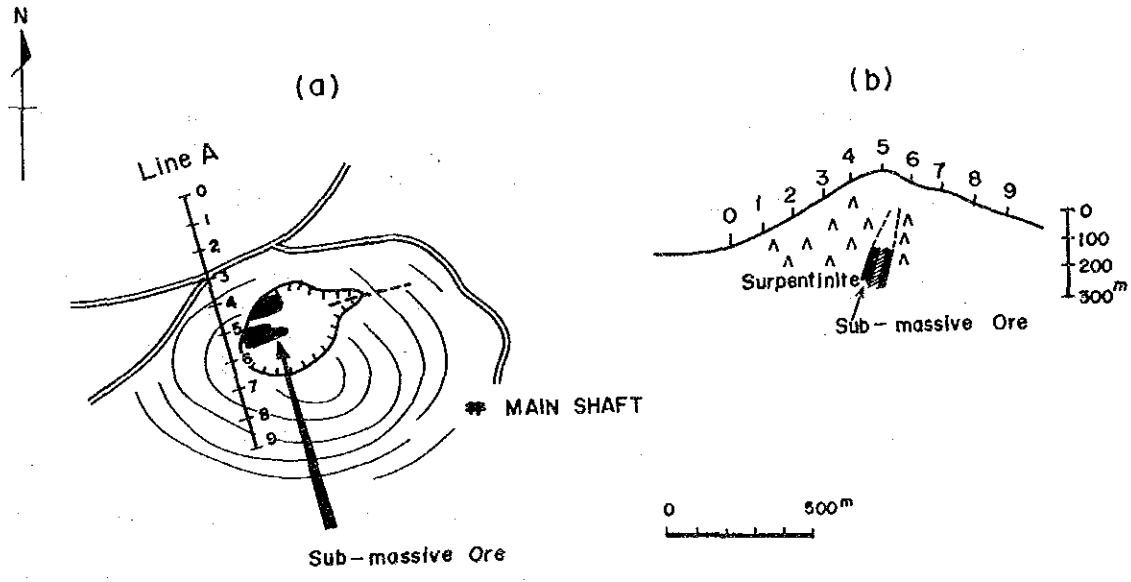

Fig · II-37 (a) Location of SIP Survey Lines
(b) Section of Line A

APPARENT RESISTIVITY (Ω-m) (0.125 Hz)

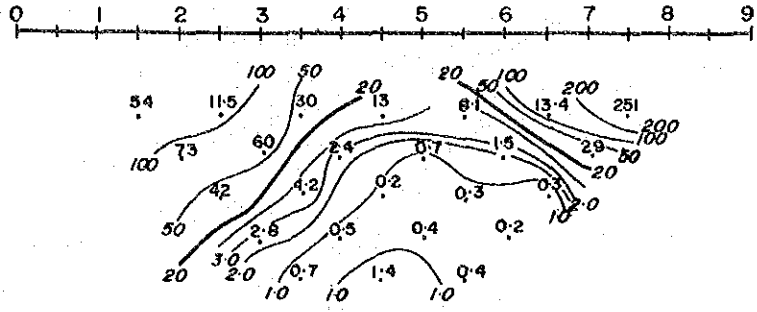

PERCENT FREQUENCY EFFECT (%) (0.125 Hz)

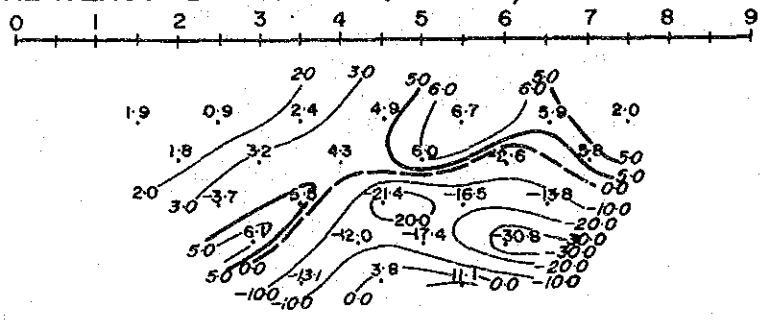

3-POINT DECOUPLING PHASE(-mad) (0.125-0.375-0.625 Hz)

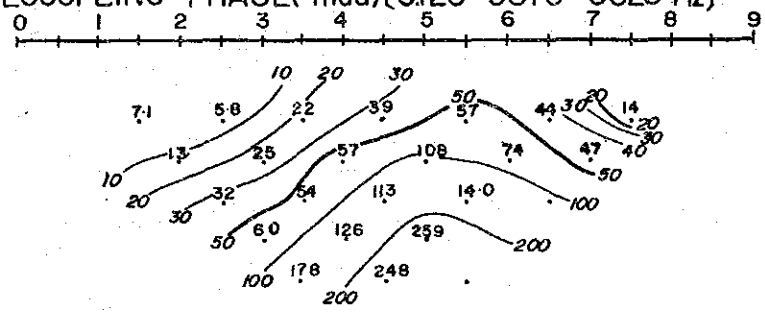

PHASE SPECTRUM

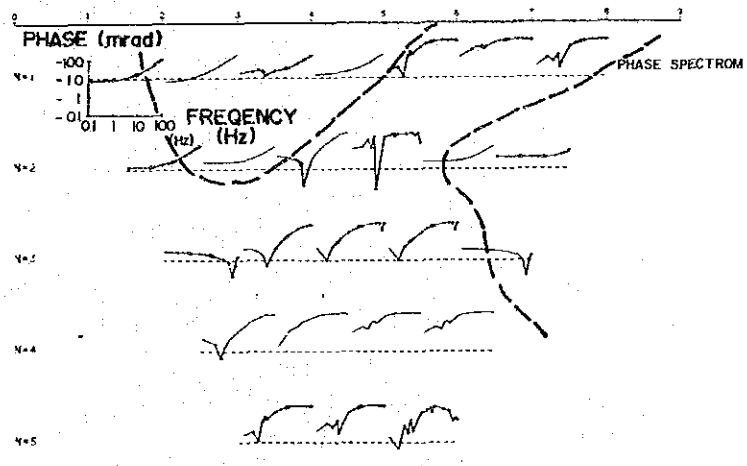

Fig II-38 Spectral-IP Pseudo-Secton Line A (Trojan Mine)

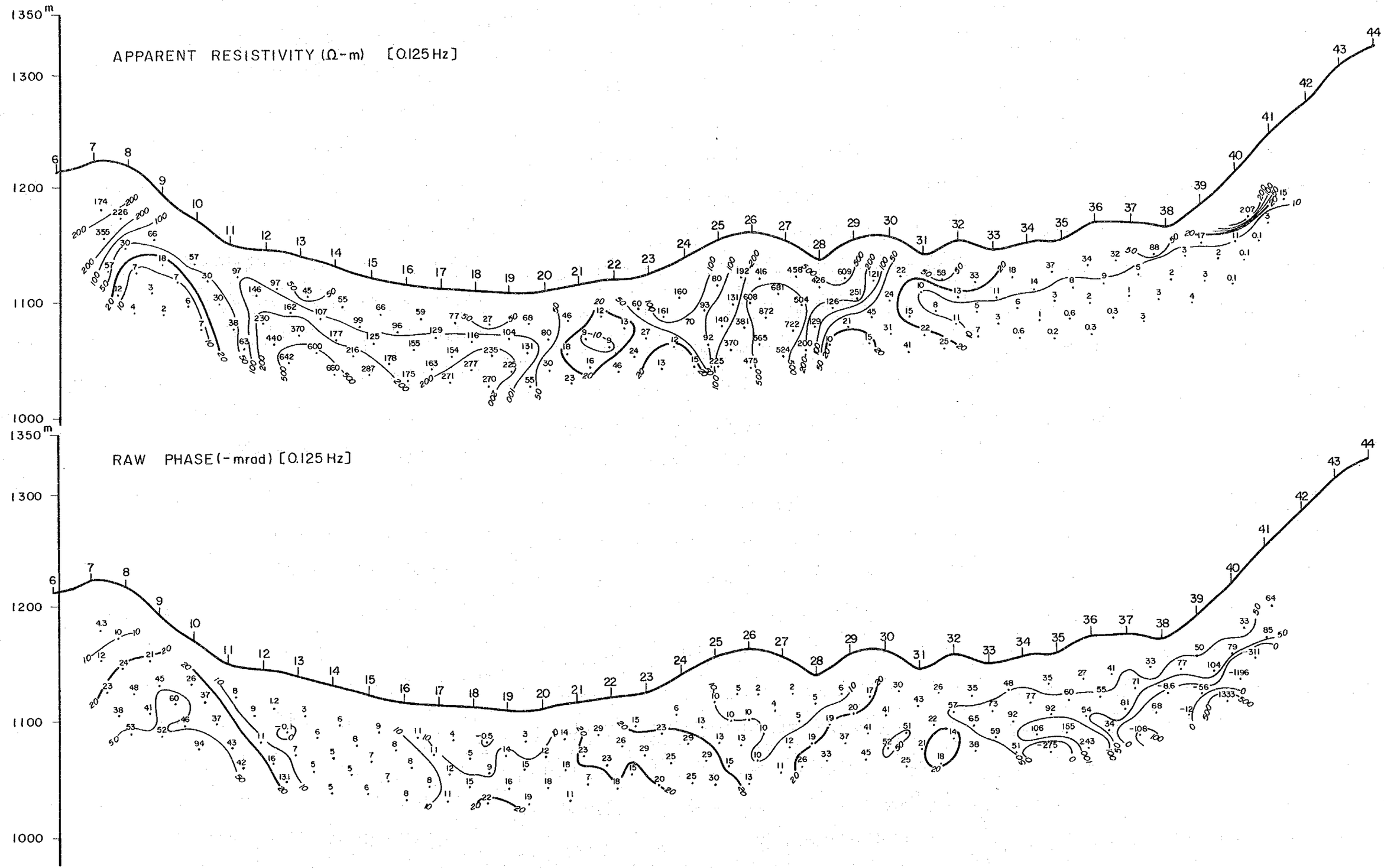

Fig. Ⅱ-39-1 Spectral IP Pseudo-Section of Line A (1)

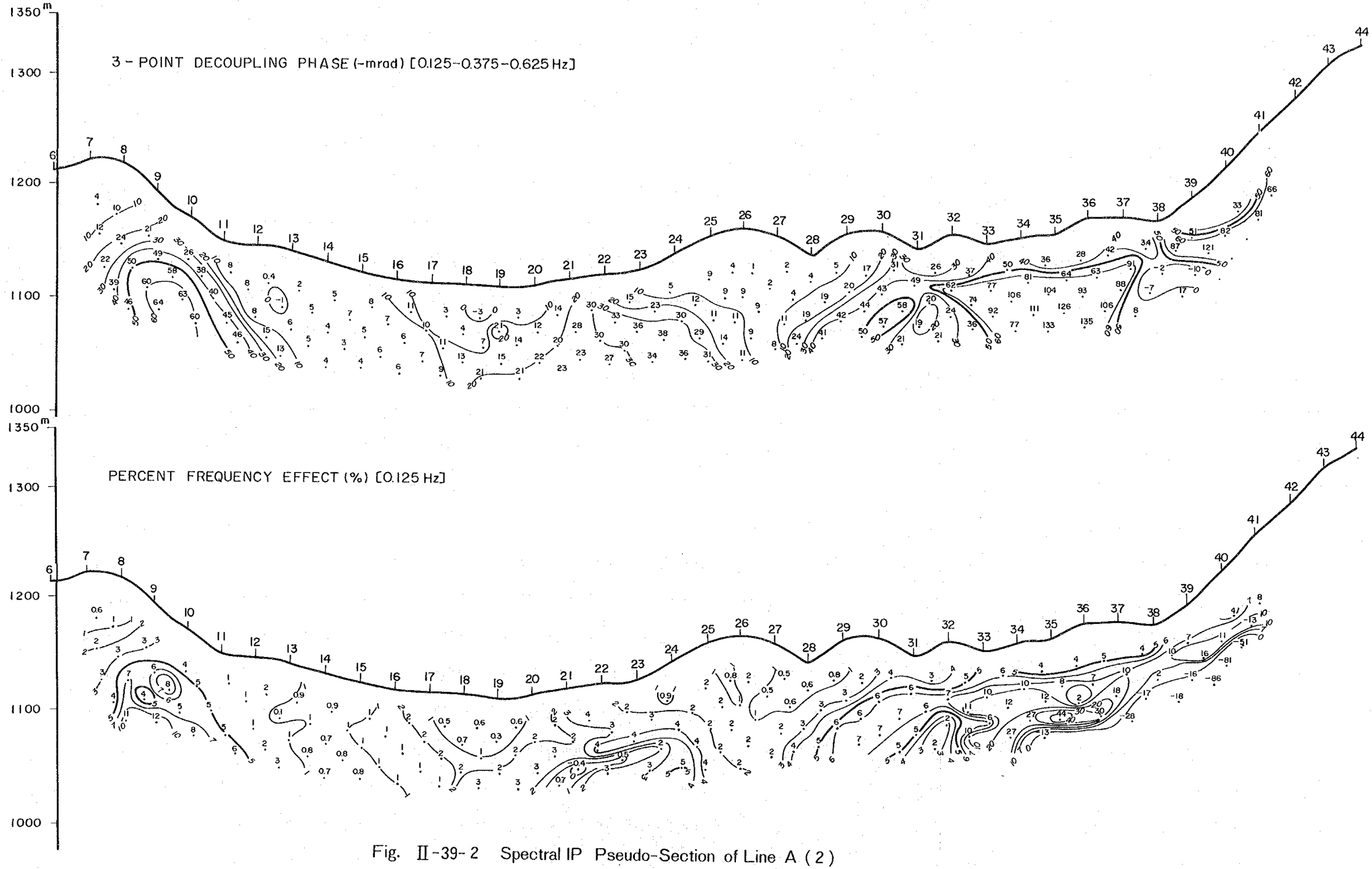

Fig. Ⅱ-39-2 Spectral IP Pseudo-Section of Line A (2)

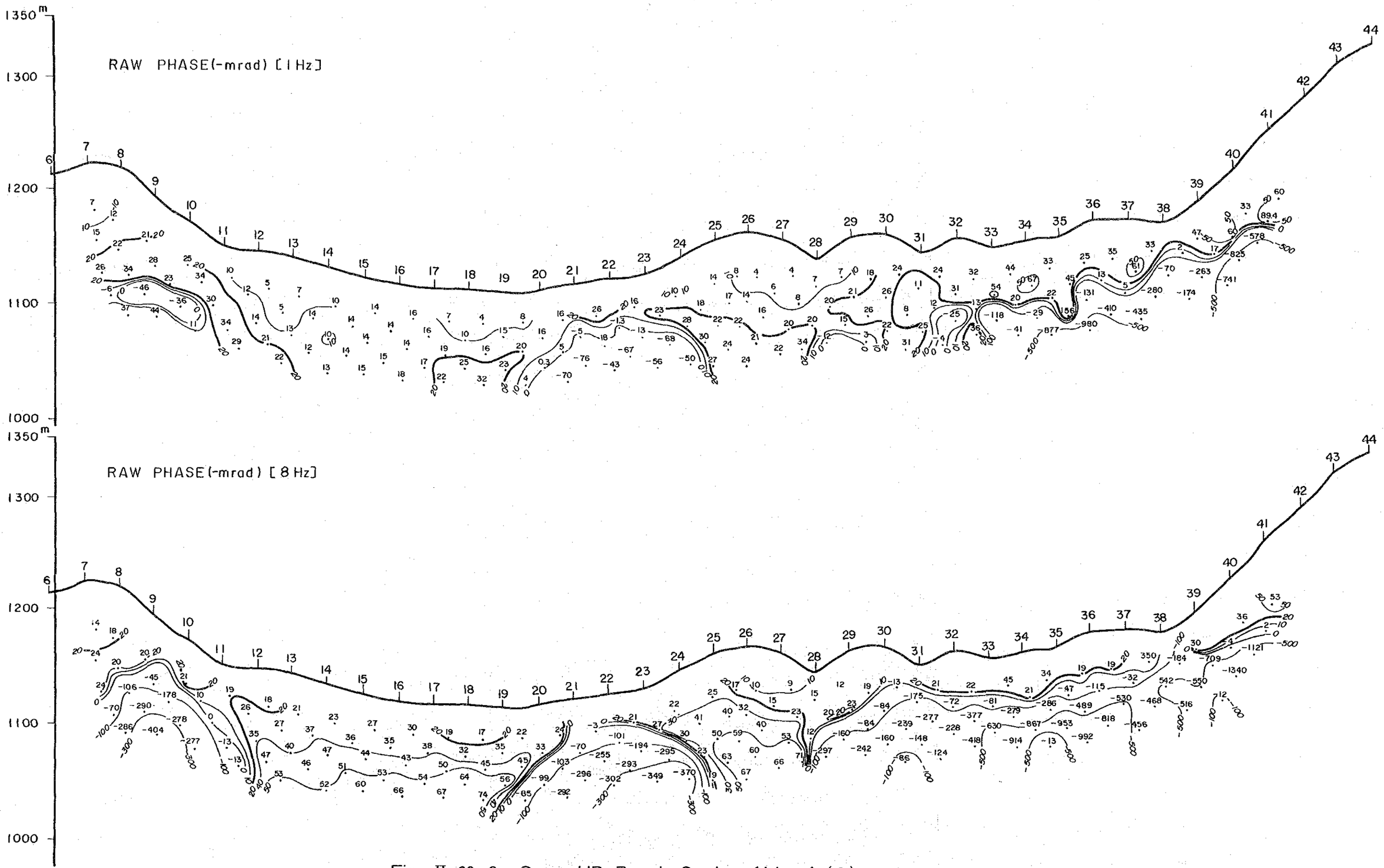

Fig. Ⅱ-39-3 Spectral IP Pseudo-Section of Line A (3)

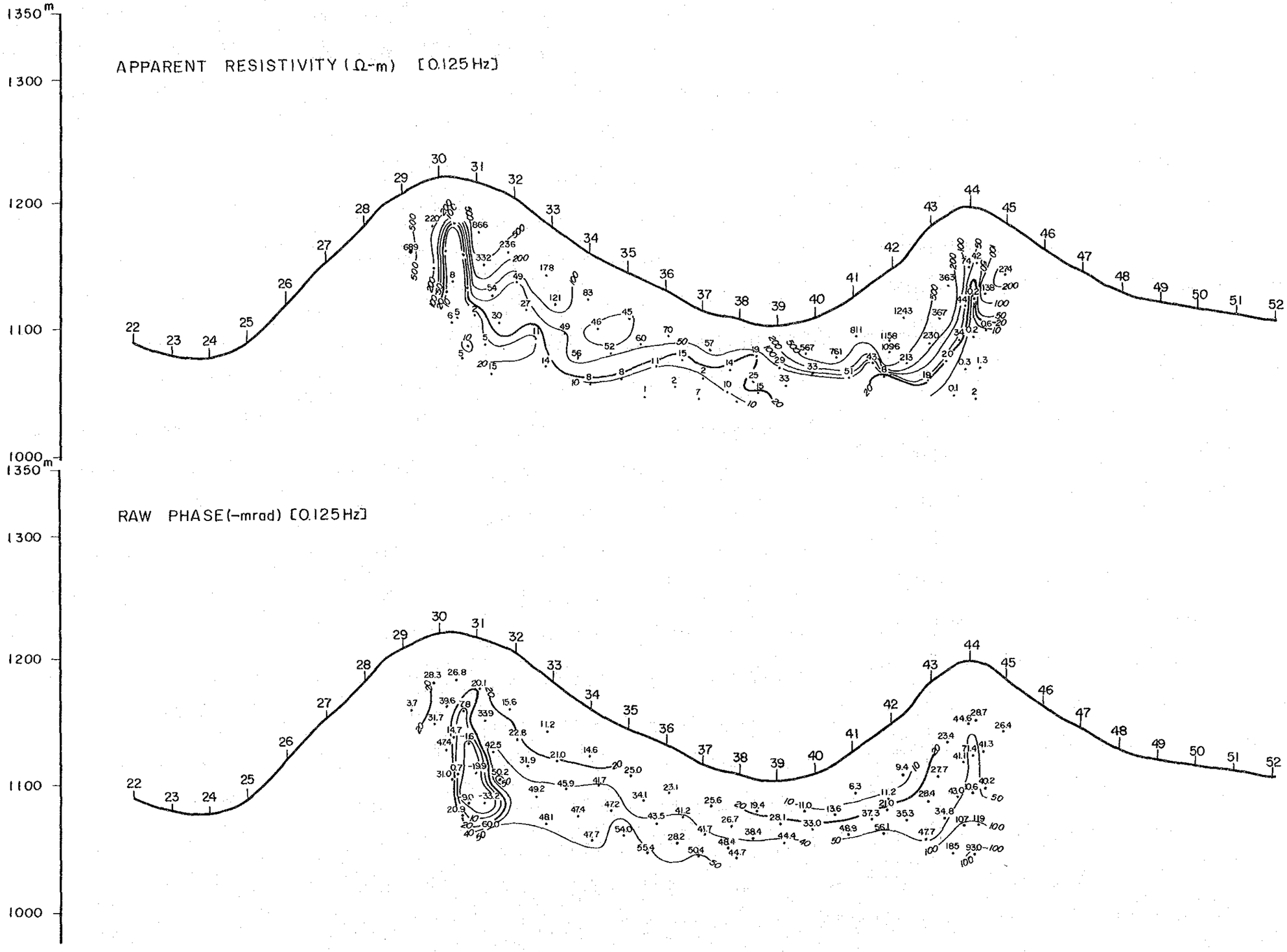

Fig. Ⅱ-40-1 Spectral IP Pseudo-Section of Line B (1)

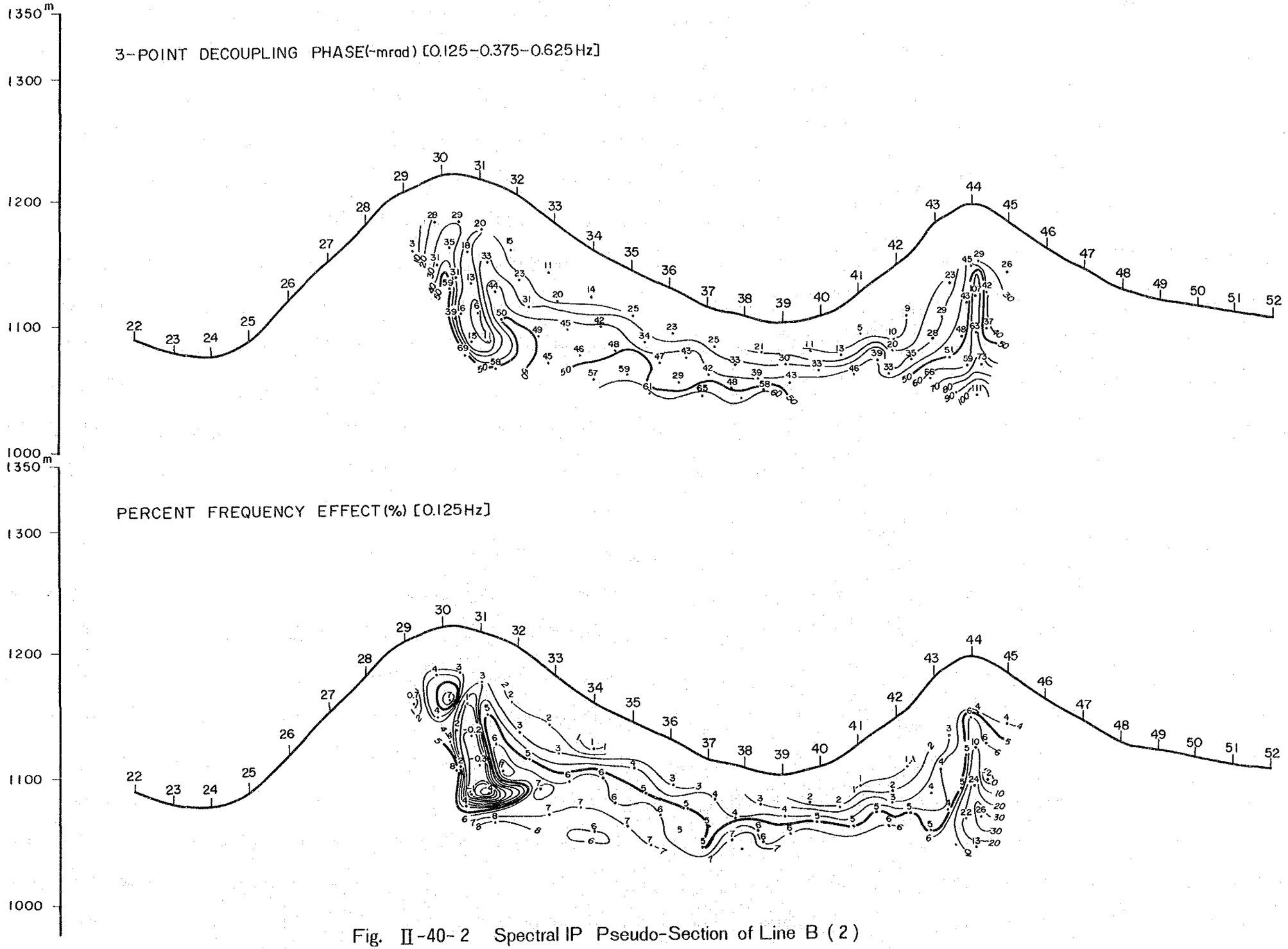

Fig. Ⅱ-40-2 Spectral IP Pseudo-Section of Line B (2)

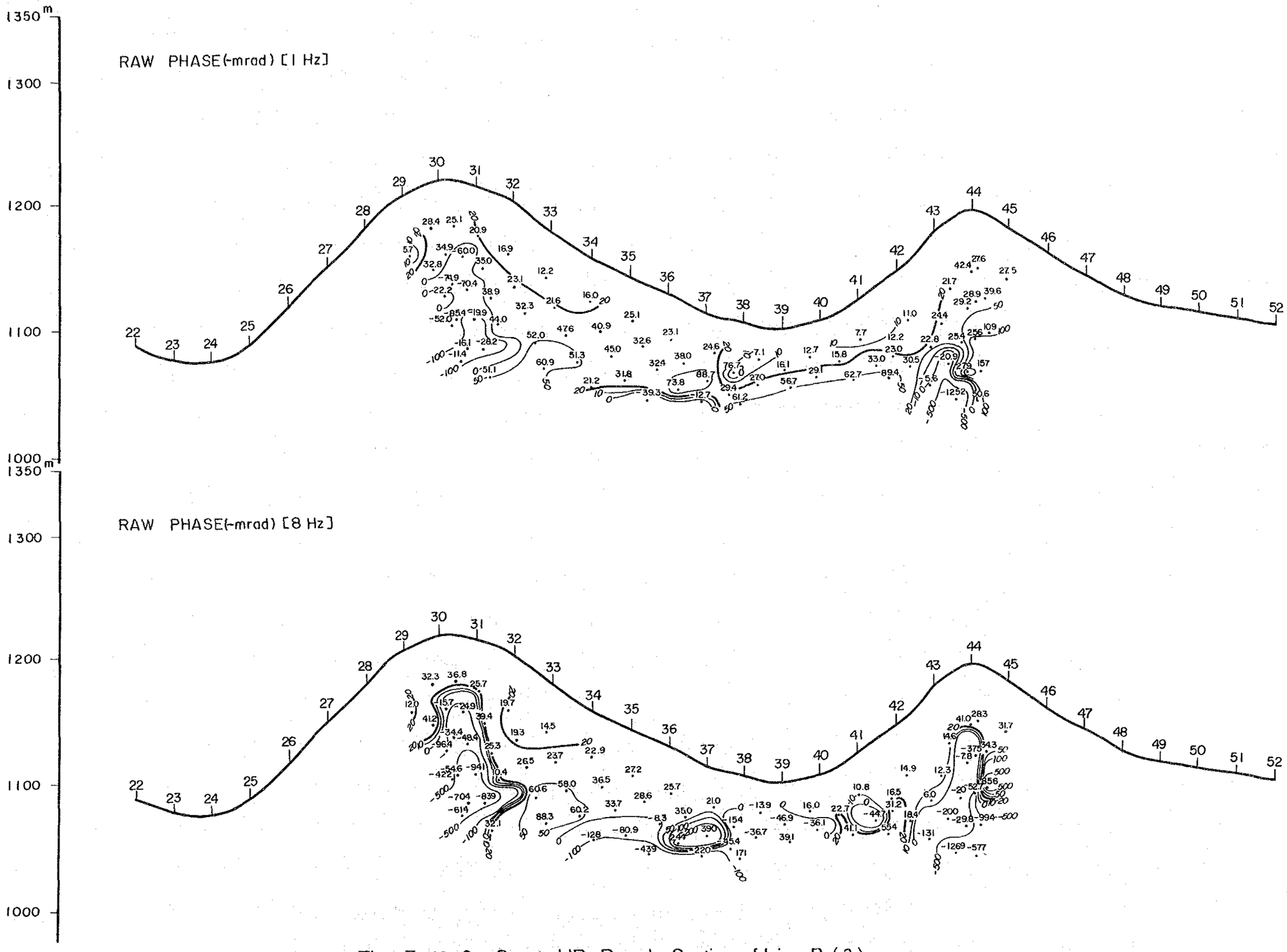

Fig. Ⅱ-40-3 Spectral IP Pseudo-Section of Line B (3)

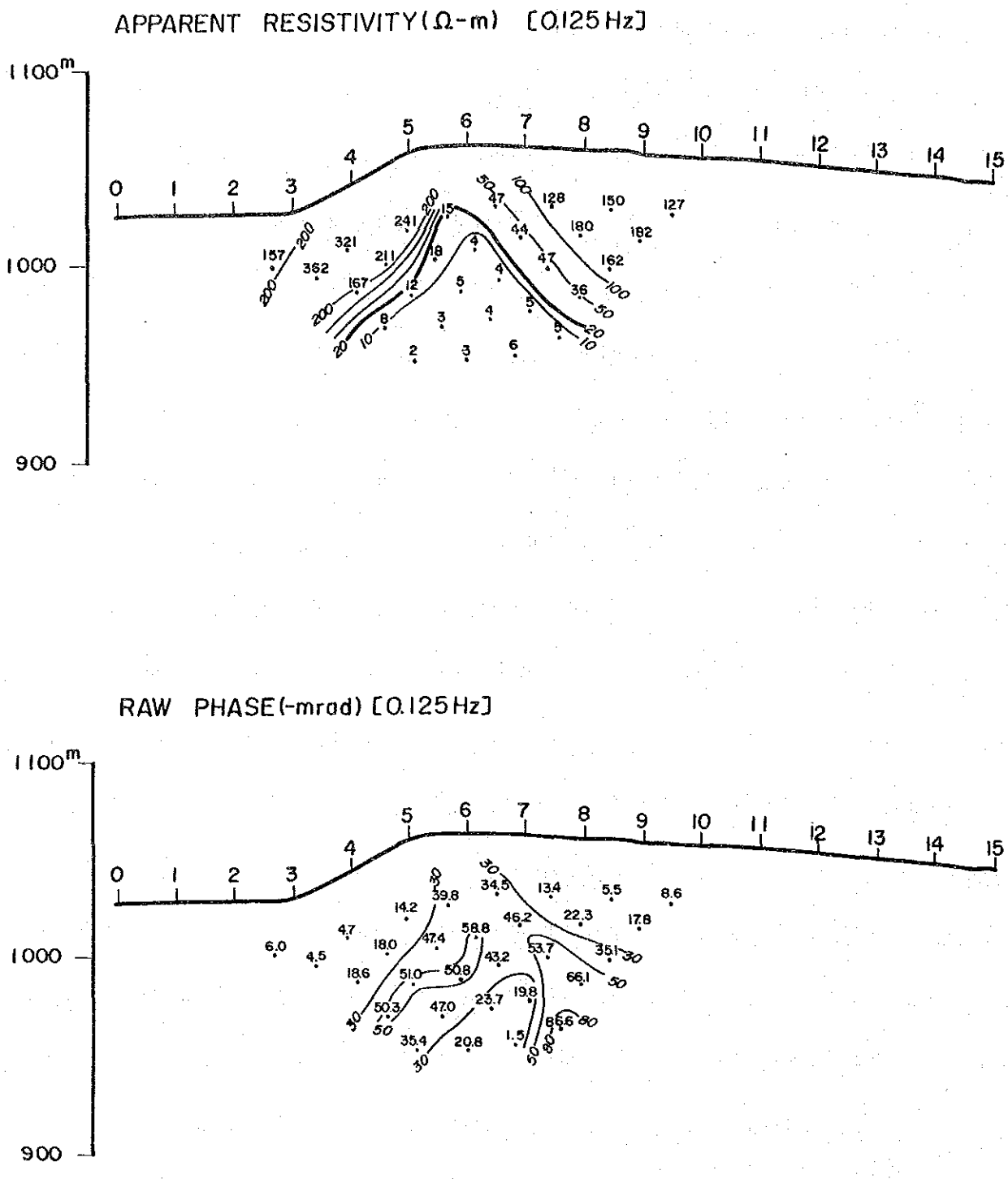

Fig. Ⅱ-41-1 Spectral IP Pseudo-Section of Line C (1)

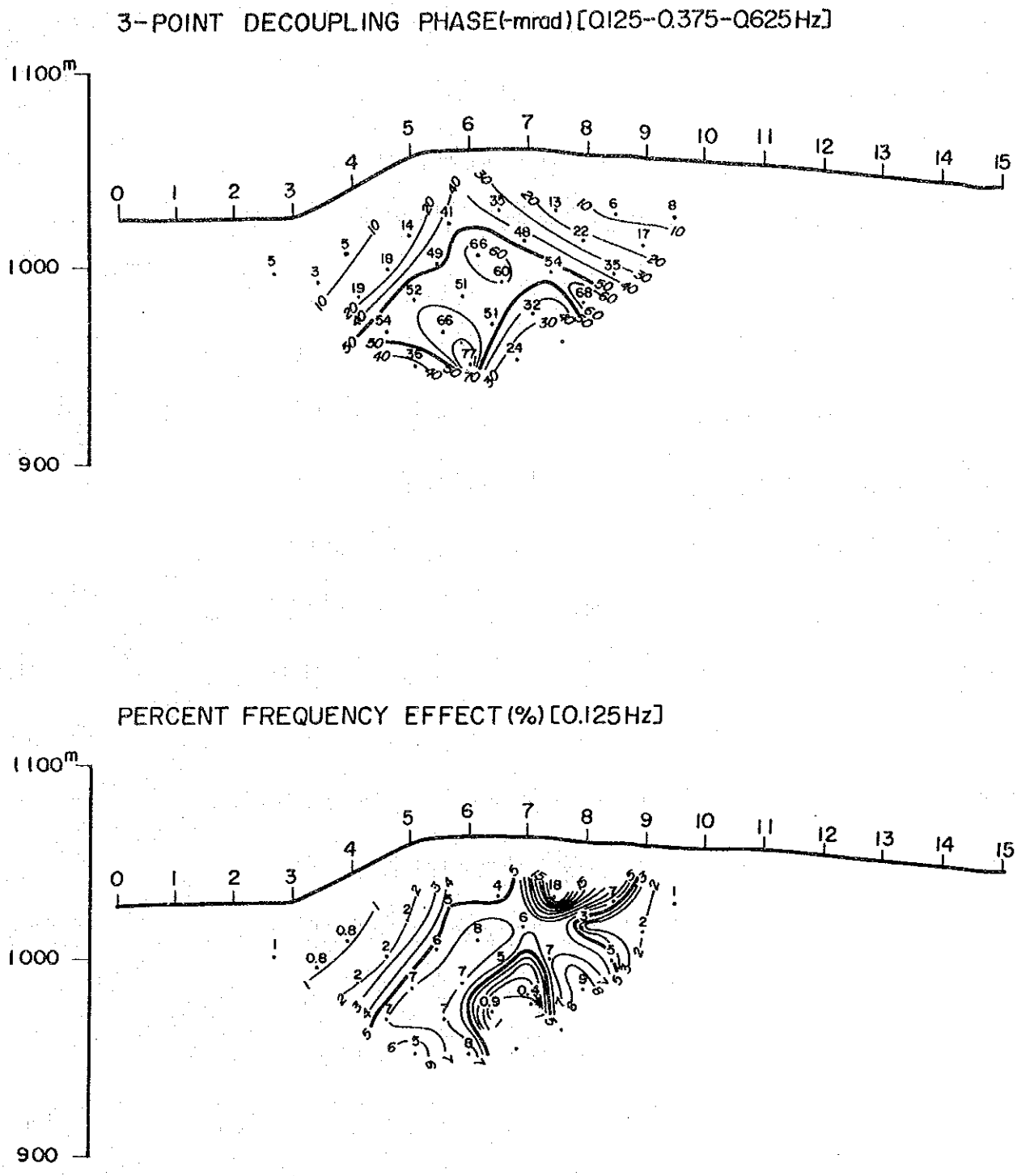

Fig. Ⅱ-41-2 Spectral IP Pseudo-Section of Line C (2)

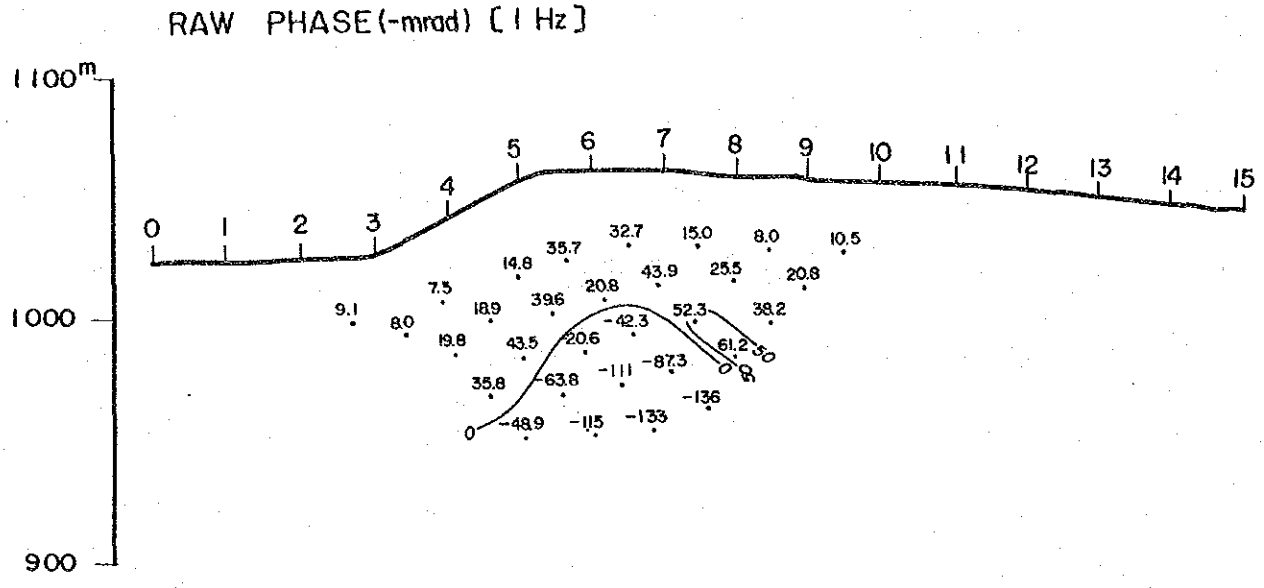

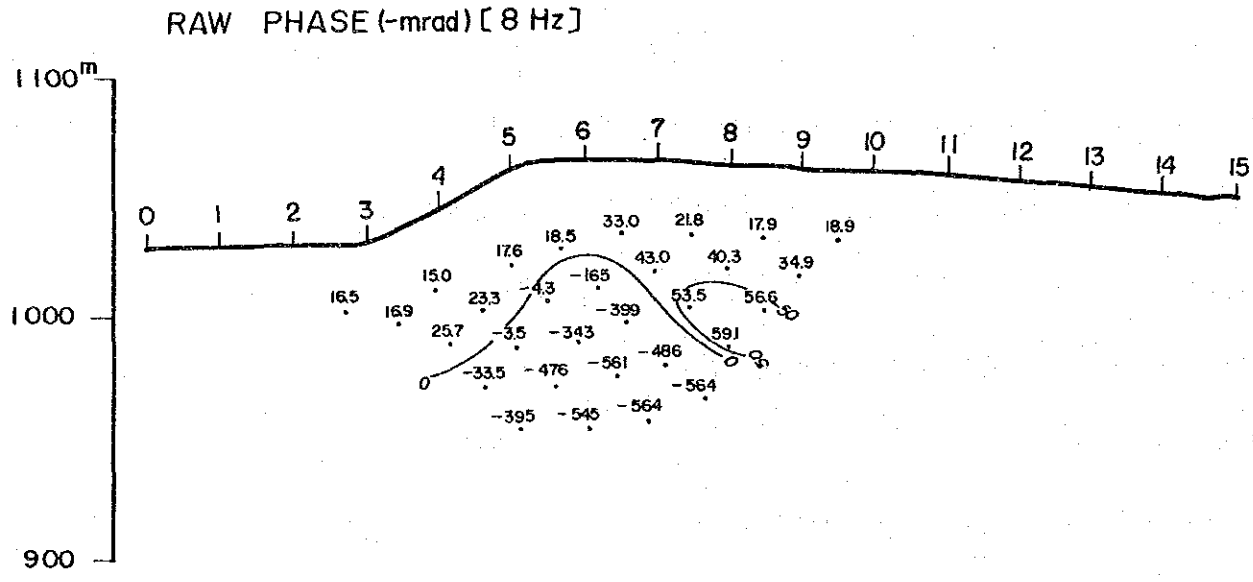

Fig. Ⅱ-41-3 Spectral IP Pseudo-Section of Line C (3)

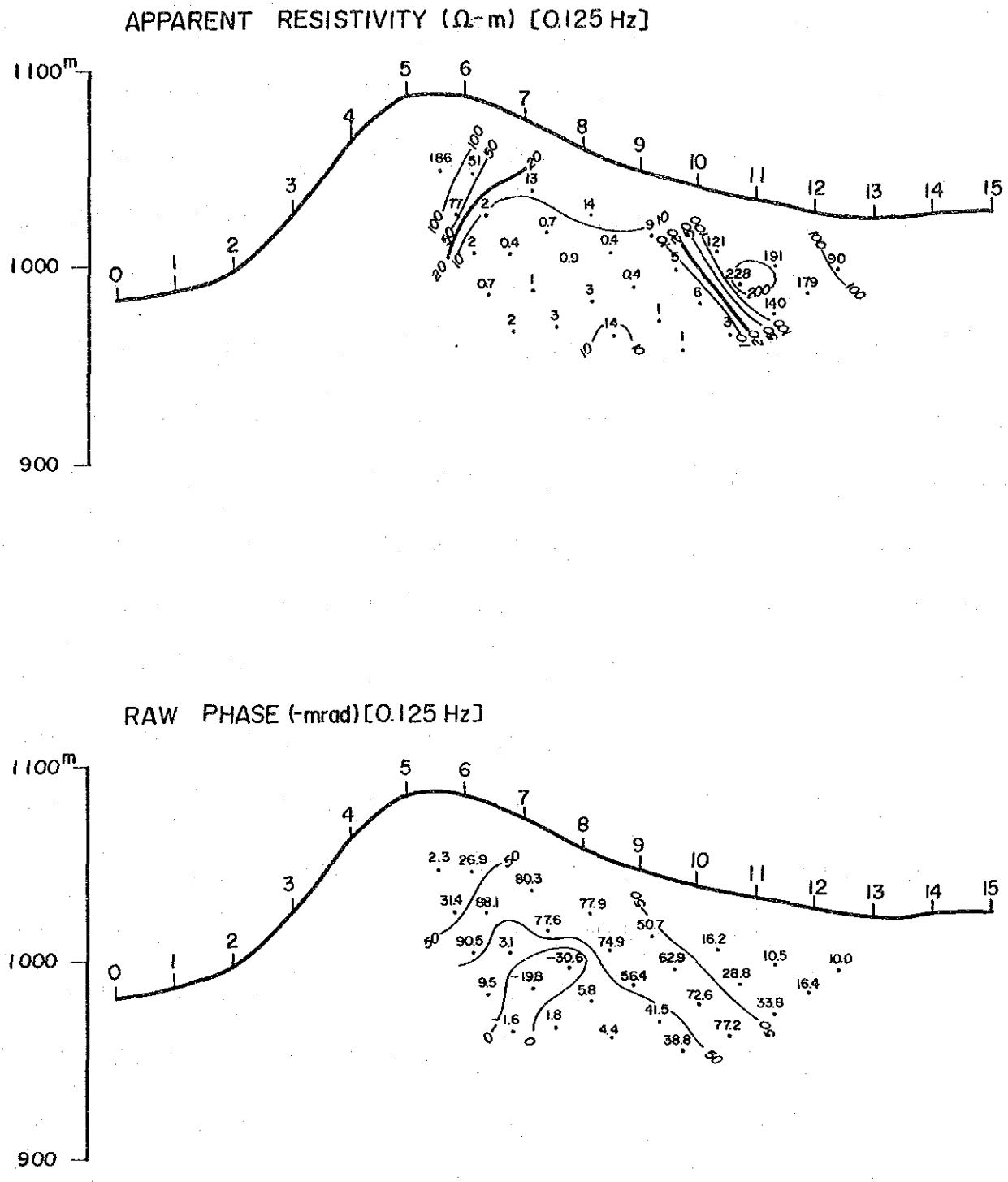

Fig. II-42-1 Spectral IP Pseudo-Section of Line D (1)

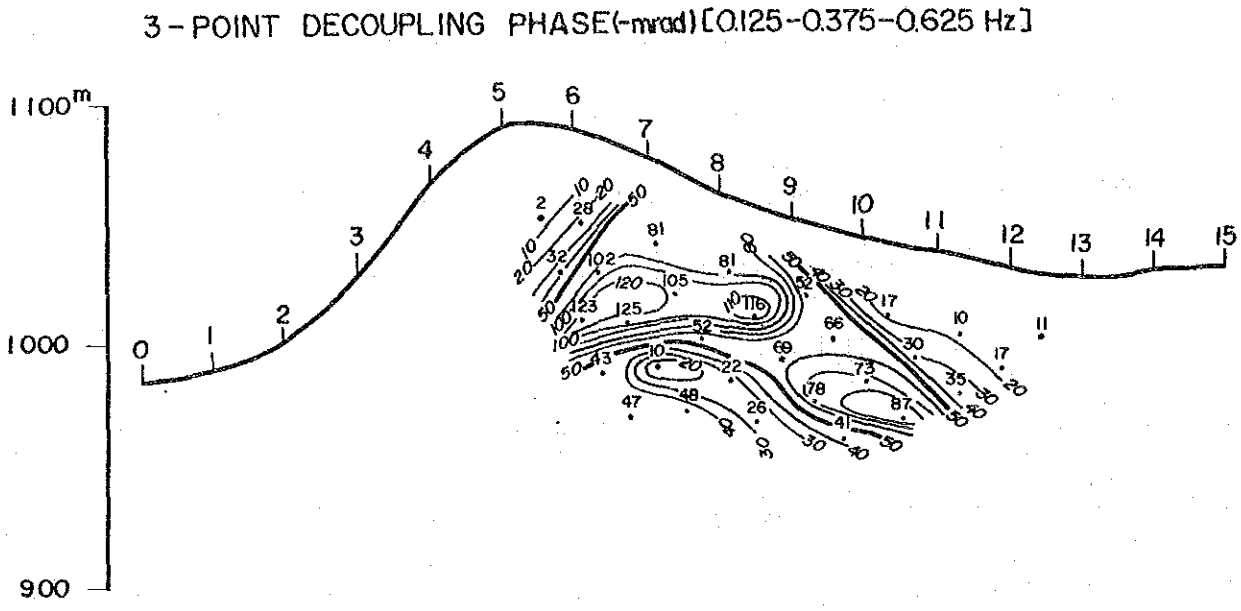

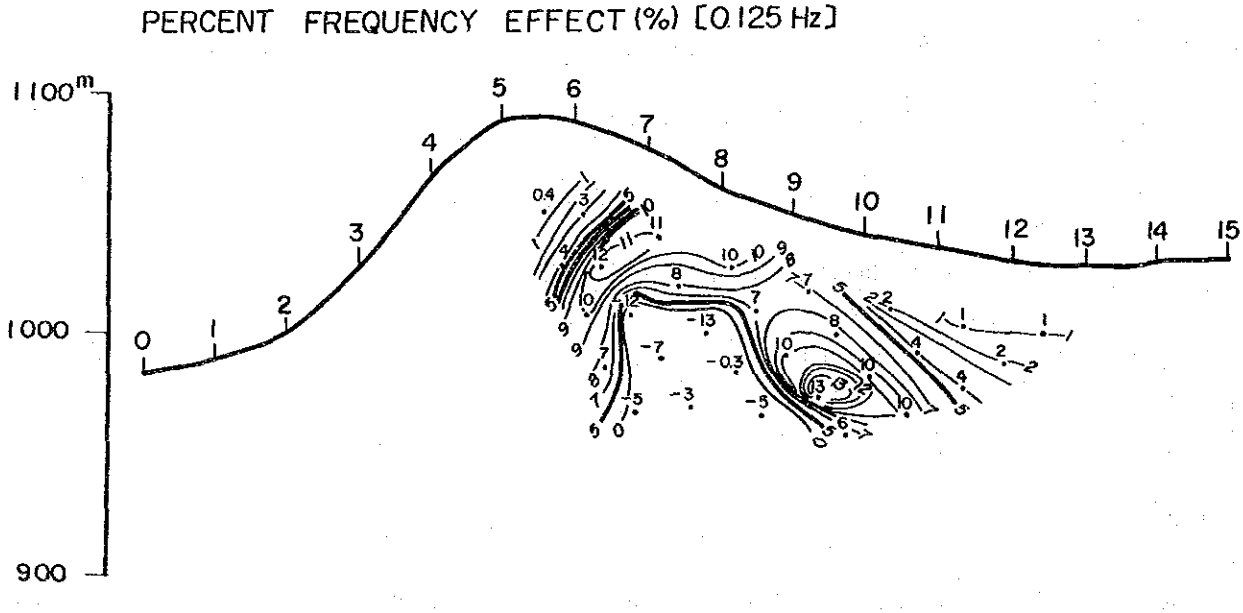

Fig. II-42-2 Spectral IP Pseudo-Section of Line D (2)

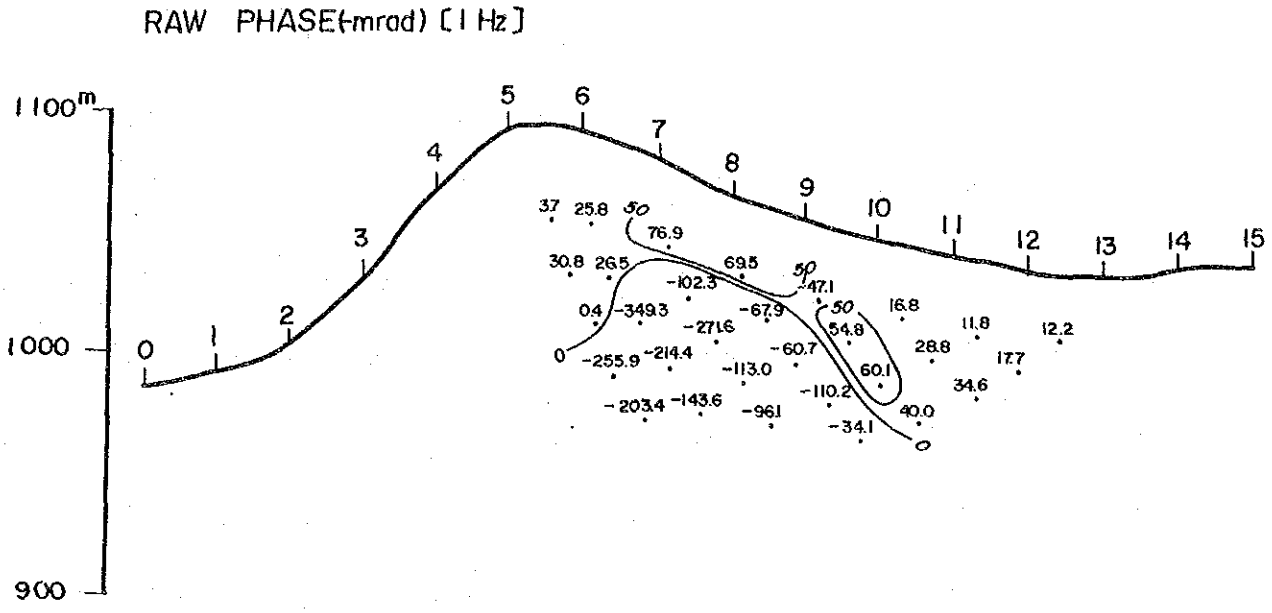

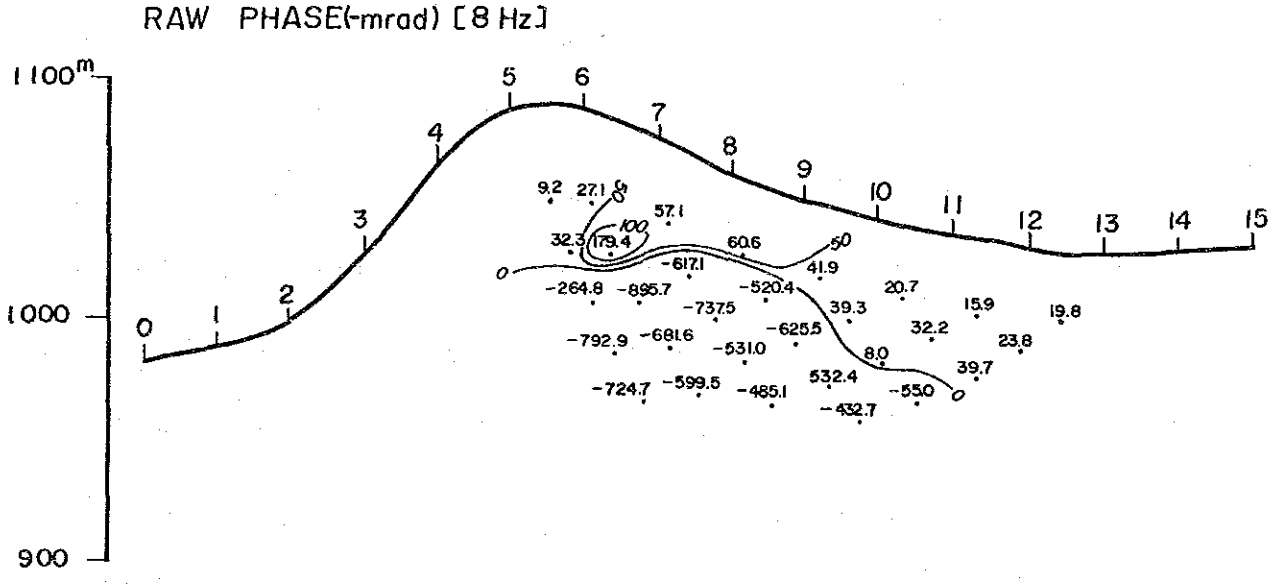

Fig. II-42-3 Spectral IP Pseuclo-Section of Line D (3)

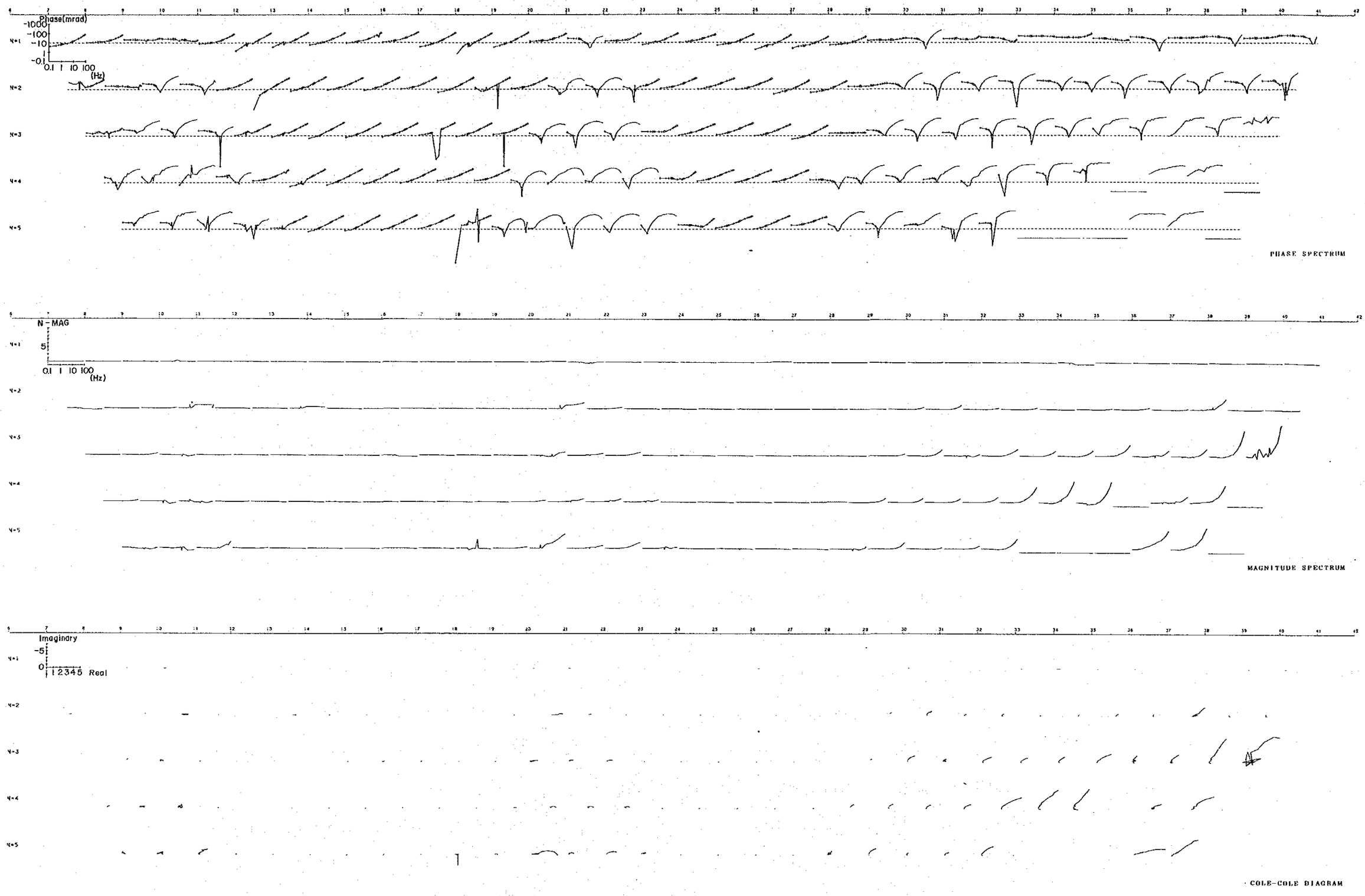

Fig. Ⅱ-43-1 Spectrum Diagram of Line A (1)

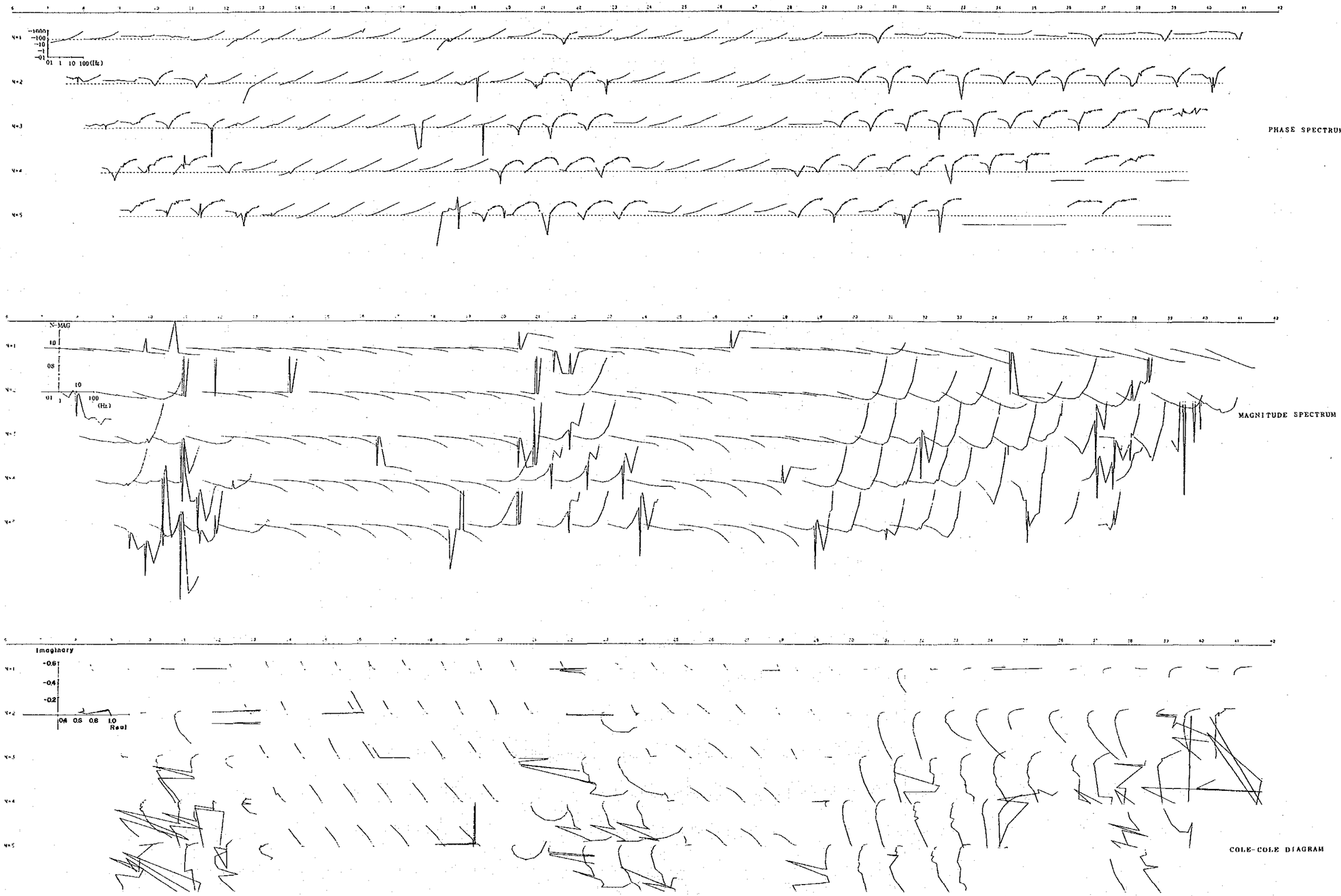

Fig. Ⅱ-43-2 Spectrum Diagram of Line A (2)

The scale of plotting is enlarged 25 times for N-MAG and Imaginary, 12.5 times for Real conponent comparing with the previous figare (1)

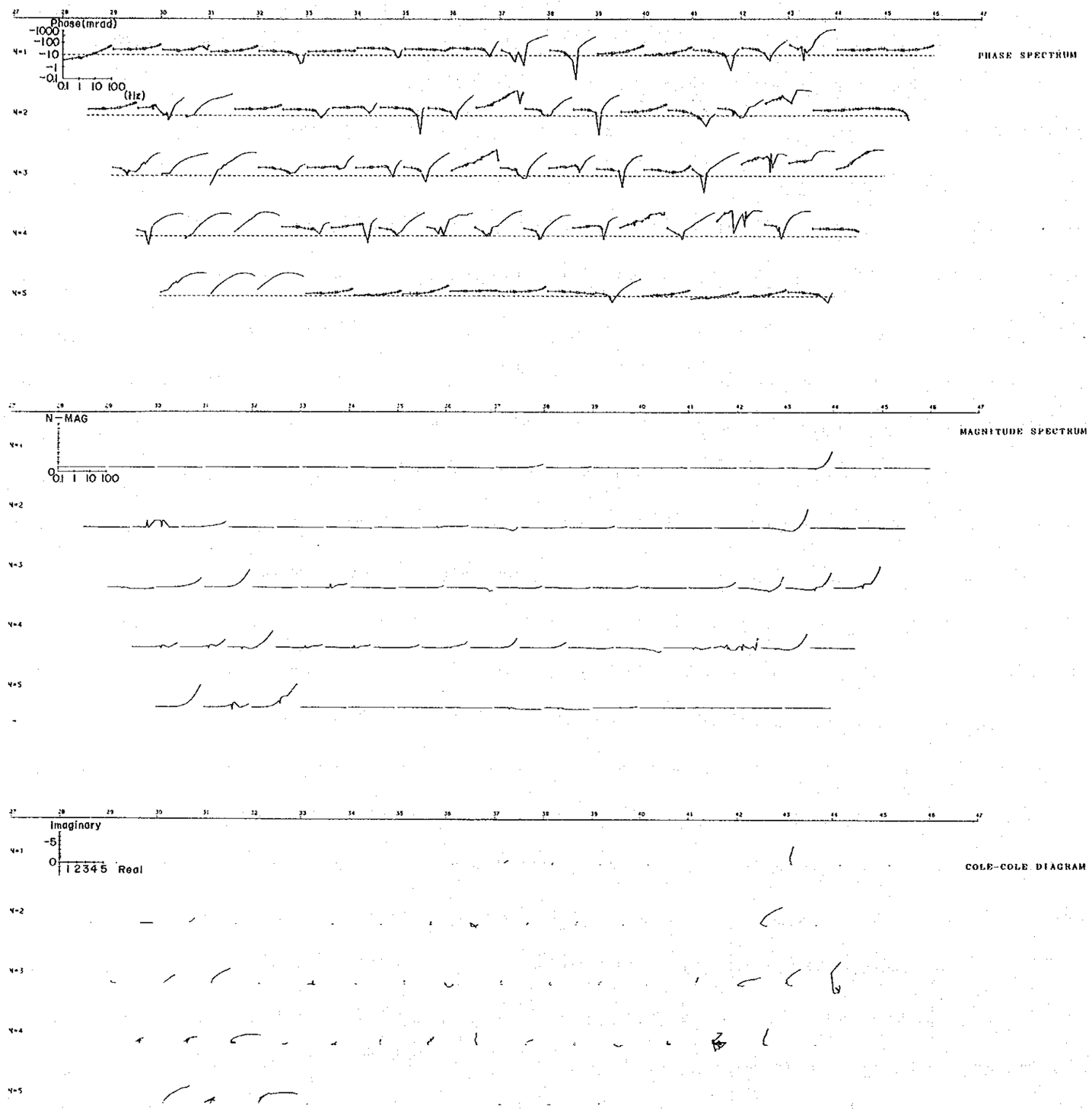

Fig. Ⅱ-44-1 Spectrum Diagram of Line B (1)

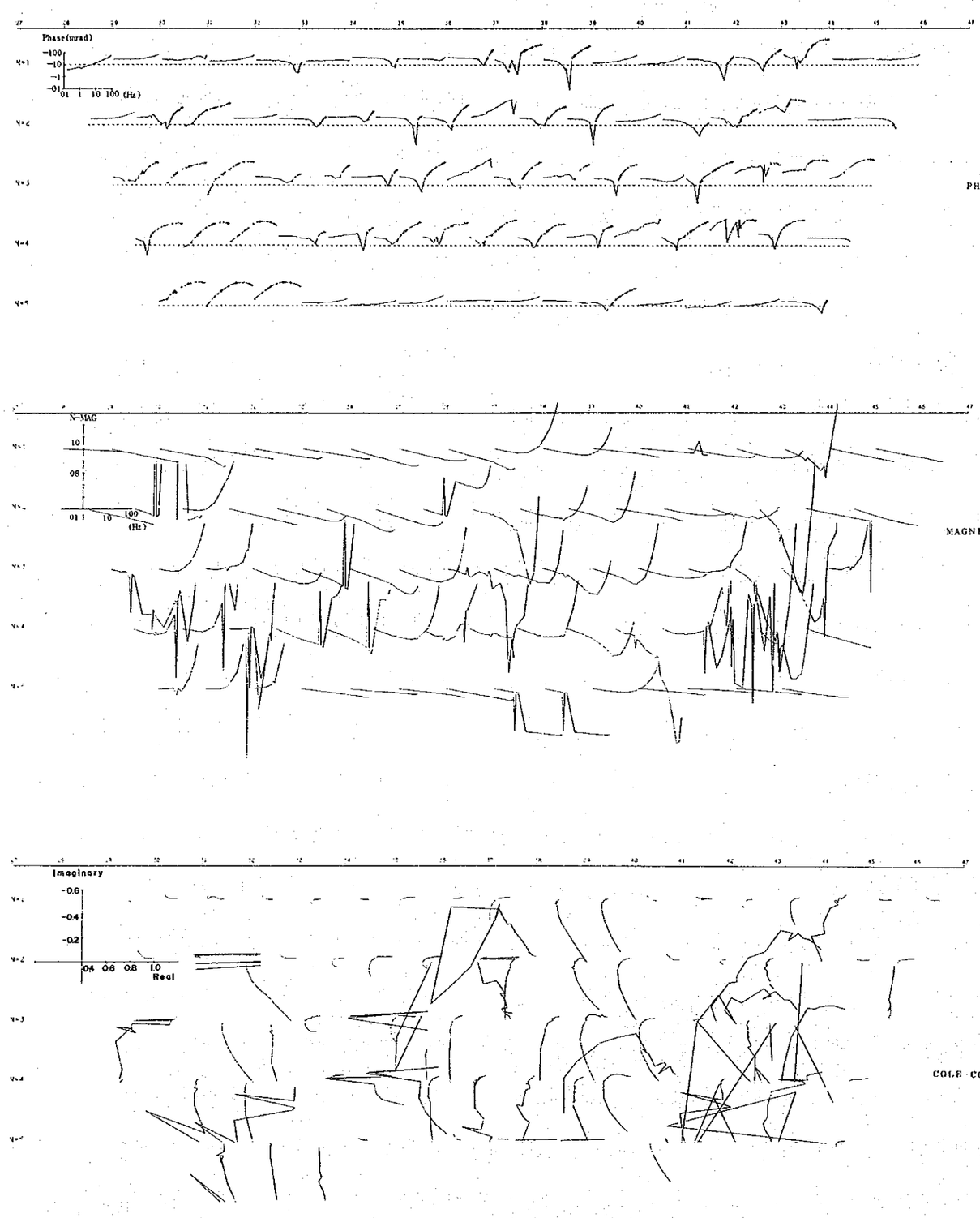

Fig. Ⅱ-44-2 Spectrum Diagram of Line B (2)

The scale of plotting is enlarged 25 times for N-MAG and Imaginary, 12,5 times for Real conponent comparing with the previous figare (1)

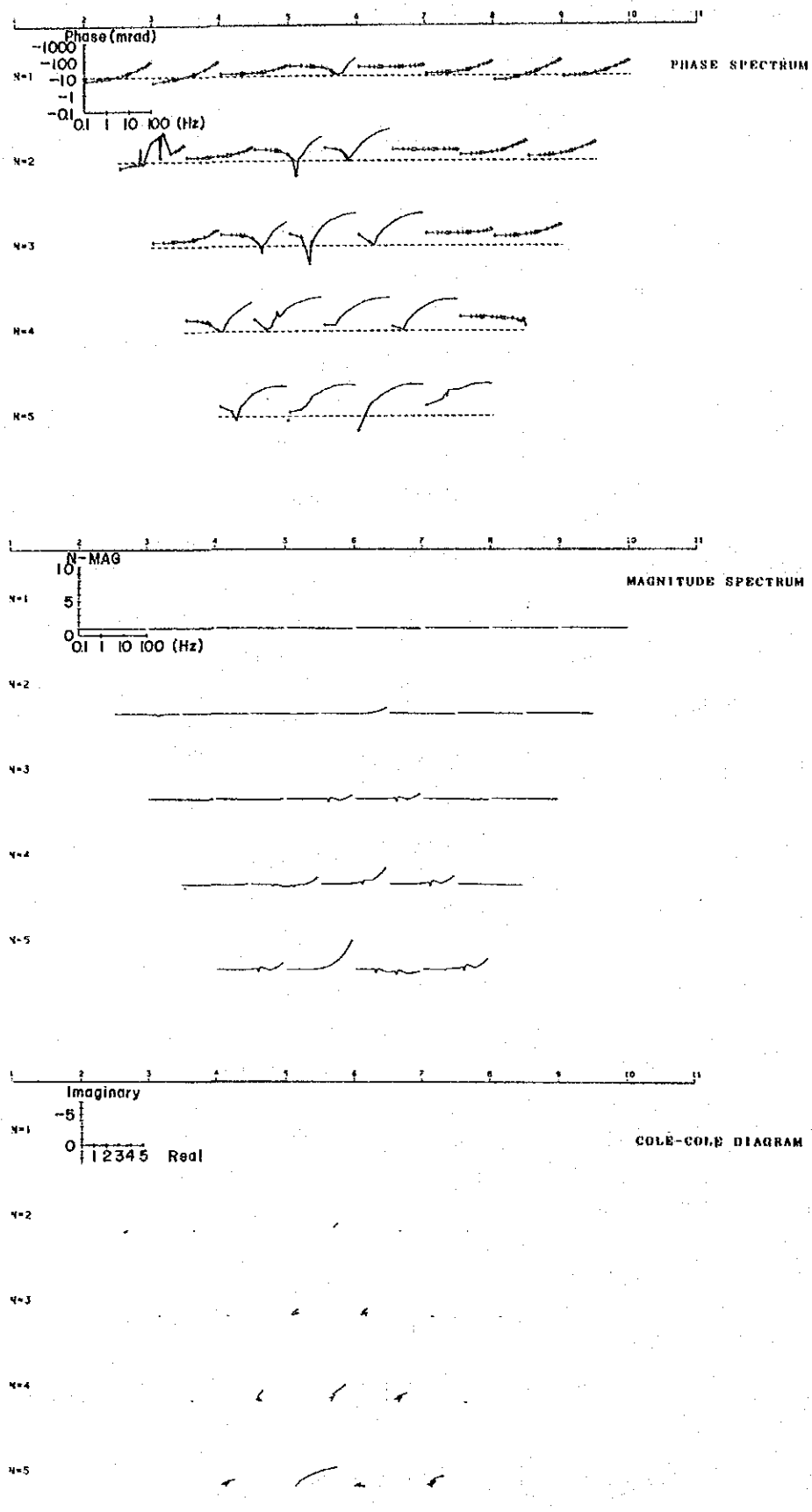

Fig. Ⅱ-45-1 Spectrum Diagram of Line C (1)

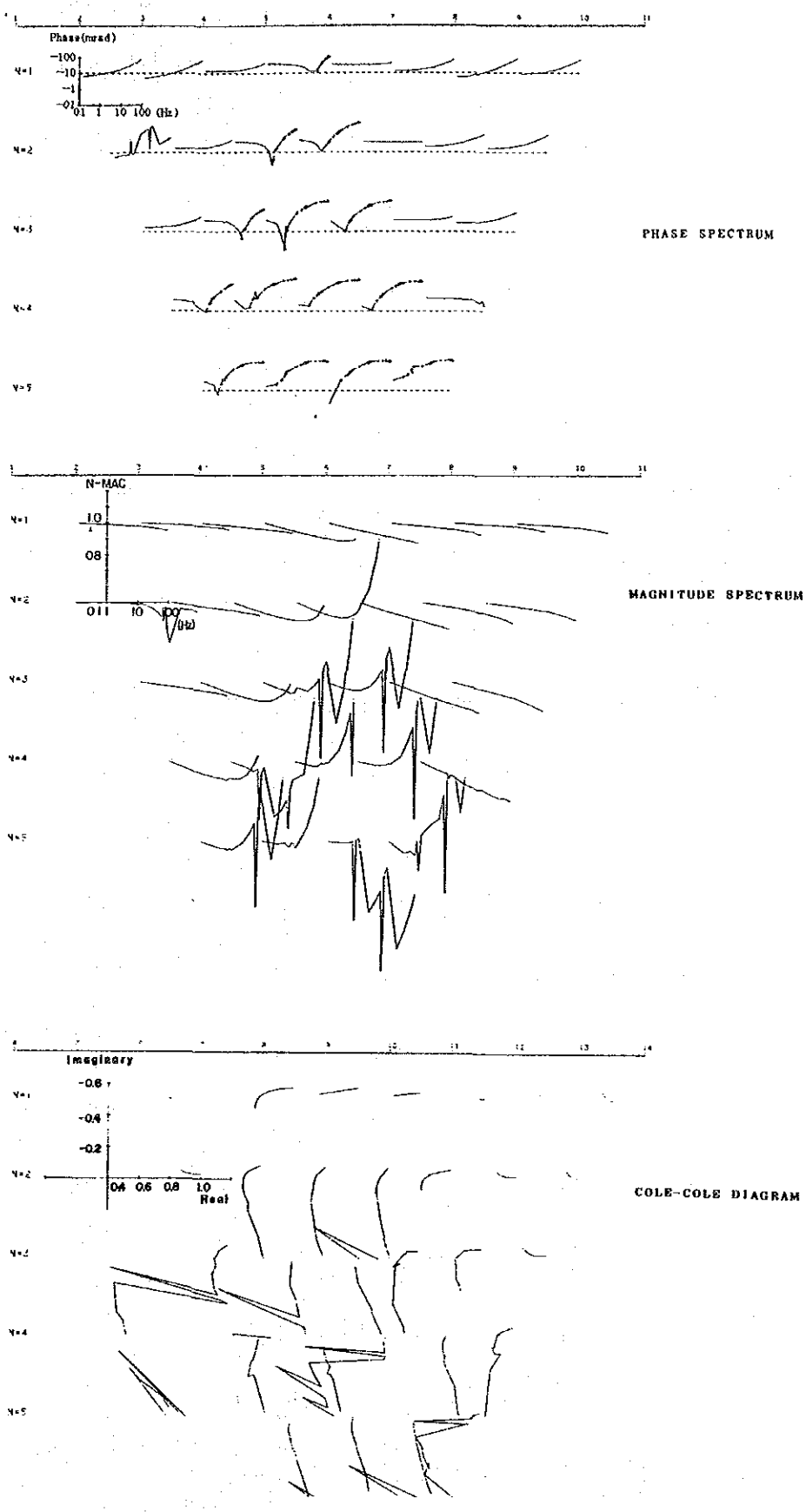

Fig. Ⅱ-45-2 Spectrum Diagram of Line C (2)

The scale of plotting is enlarged 25 times for N-MAG and Imaginary, 12.5 times for Real conponent comparing with the previous figare (1)

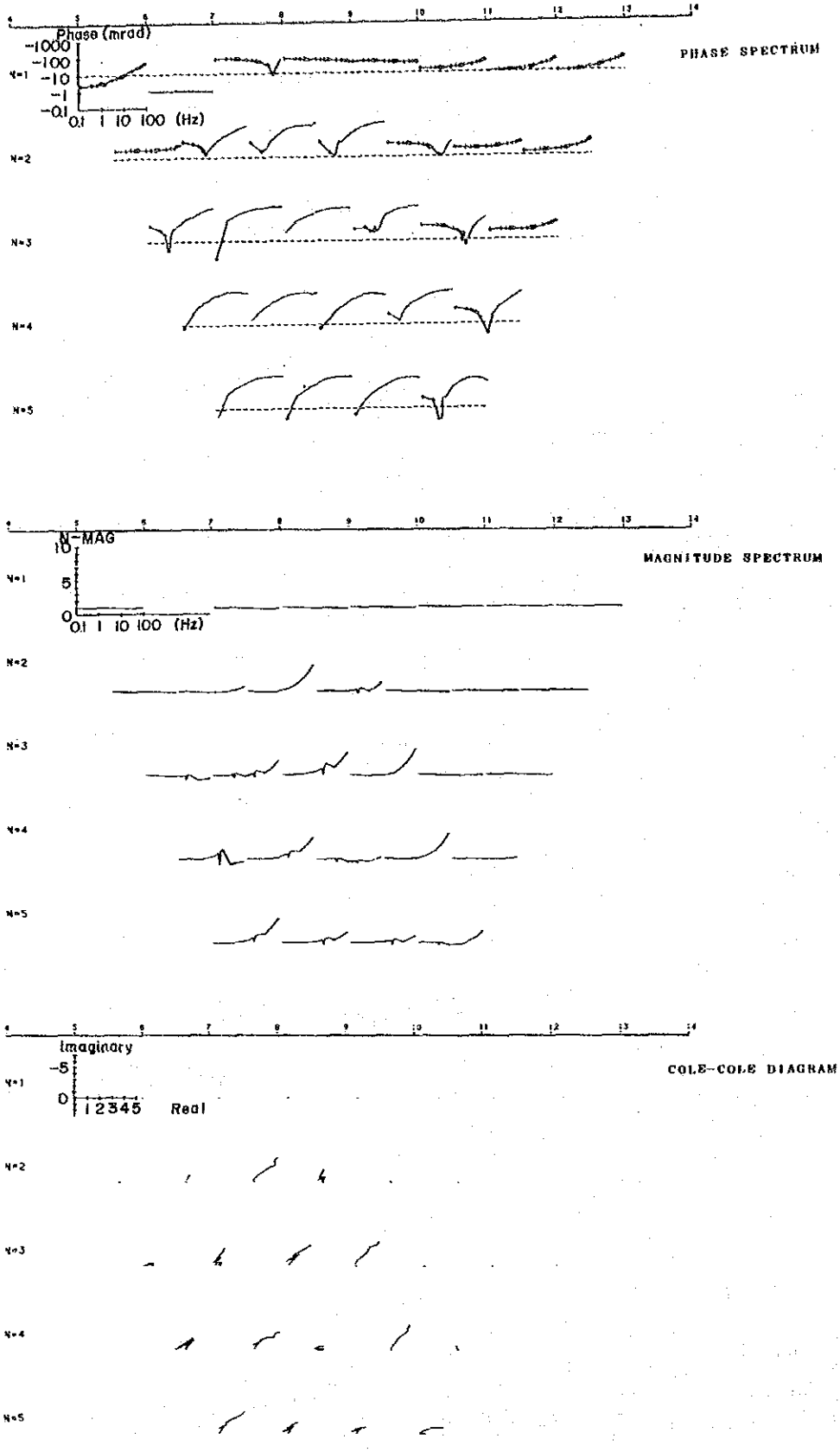

Fig. Ⅱ-46-1 Spectrum Diagram of Line D (1)

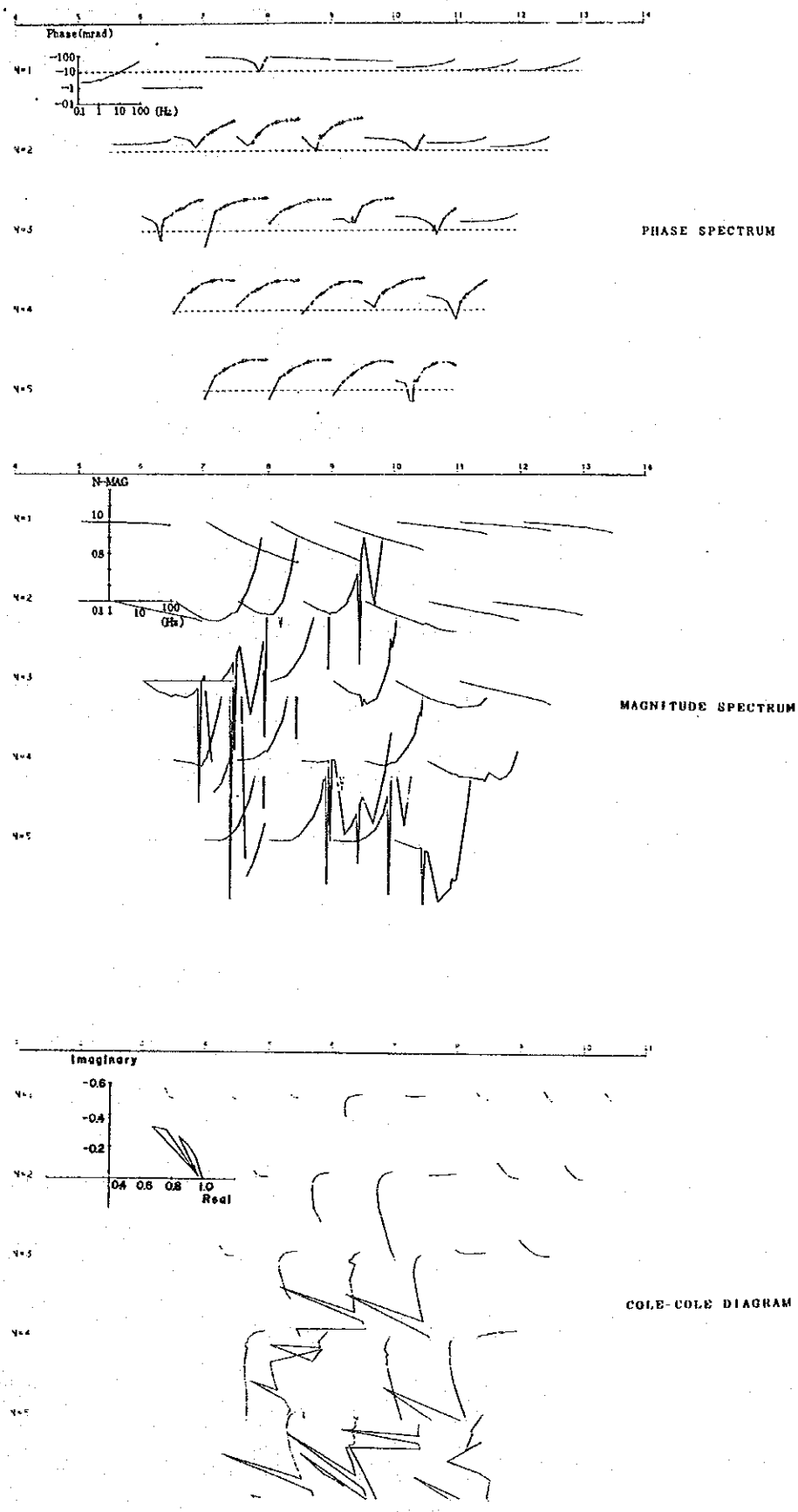

Fig. Ⅱ-46-2 Spectrum Diagram of Line D (2)

The scale of plotting is enlarged 25 times for N-MAG and Imaginary, 12.5 times for Real conponent comparing with the previous figare (1)

PART 3
SYNTHETIC ANALYSIS

SYNTHETIC ANALYSIS

The results of the synthetic analysis of all the geological, geochemical, and geophysical survey data, collected for the past two years, are as follows.

Area C

The low resistivity zone around C-81-0 to C-86-0 (in the southern rim of the area) which was detected by the CSAMT survey, is deep, but located in an unfavourable geological setting for nickel sulphide ore deposits. Rocks in the area are andesite, chert, and banded ironstone.

The Trojan ore horizon, which contains serpentine intrusive bodies, extends to about 600m to 800m north of the low resistivity zone. A geochemical anomaly covers the extension zone of the Trojan ore horizon, but does not cover the low resistivity zone. Judging from this evidence, no further geophysical survey is recommended for this zone.

The low resistivity zones around C-82-9 and C-89-6 are located near a serpentine body in the Trojan ore horizon extension, and are associated with a geochemical anomaly. But, their size and depth are poor. No further geophysical survey is also recommended for these zones.

Area D-1

The low resistivity zones around D-41-6, D-39-12, D-38-6, D-33-6, and D-30-9, which were detected by the CSAMT survey, are located on a serpentine body in the extension zone of the Trojan ore horizon in the north-south central part of the area. Their depth extension is also good. Among them, D-41-6 and D-38-6 coincide with the distribution of pegmatite dykes. This is an inconsistent phenomenon, because, generally, pegmatites show high geophysical resistivity. It might indicate that these pegmatite dykes are

small scale, with poor depth extension.

The zones of D-41-6, D-39-12, and D-33-6 are not coincident with any geochemical anomaly, but the zones of D-38-6 and D-30-9 are coincident with strong geochemical anomalies. The latter two zones extend to depth, and their scales are extensive. Therefore, the potential for expected sulphide ore deposits associated with serpentines is high, and further geophysical survey, SIP, was recommended for them.

The IP anomalies around D-36-4 to D-36-8 and D-30-6 to D-30-11, found in SIP survey lines "C" and "D" are deep-sited and strong. They are expected to be caused by nickel sulphides associated with serpentines. It is therefore recommended that a drilling program be conducted to examine the existence of mineralized zones.

Area D-2

The low resistivity zones around D-3-12 and D-8-18, which were detected by the CSAMT survey, are on the eastern side of a serpentine body in the extension of the Trojan ore horizon, the local rocks are banded ironstones. The zones extend to depth, but are not coincident with any geochemical anomaly. In spite of this evidence, the D-8-18 zone was covered by a SIP survey line in relation to the low resistivity zones detected by the CSAMT survey in Area D-3.

The IP anomaly around D-7-10, which was found in the SIP survey line "A", is a deep-sited one, located near a serpentine body. It is expected to be caused by nickel sulphides associated with serpentines, and it is recommended that a drilling program be conducted to examine the existence of mineralized zones, despite the lack of an associated geochemical anomaly.

Area D-3

The low resistivity zones around D-4-33, D-7-36 to D-7-42, and D-9-39 to D-9-42, which were detected by the CSAMT survey, are on a serpentine body surrounding banded ironstones, in the extension of the Trojan ore horizon. A geochemical anomaly is coincident with this serpentine body, and closely associated with the low resistivity zones. Depth extension of the zones is good.

Among them, the zone D-10-39 to D-9-42 is well known as the Tynan Occurrence. Extensive exploration programs have been conducted by companies several times, including drilling programs. Therefore, this zone was eliminated from the SIP survey target. The rest are in a favourable geological setting and coincident with geochemical anomalies. Further SIP survey was therefore recommended for them.

The IP anomaly around D-7-35, which was found in the SIP survey line "A", is strong, deep-sited, and is, located in the southwestern extension, about 600m, from the Tynan Occurrence, in the eastern rim of the serpentine body. This strongly suggests that the anomaly is caused by nickel sulphides associated with the serpentine. It is therefore recommended that a drilling program be conducted to examine the existence of mineralized zones.

The IP anomaly around D-4-44, which was found in the SIP survey line "B", deviates from the serpentine body, and geochemical anomalies. Rocks around here are banded ironstones and cherty sediments. But because this good IP anomaly exists in association with a low resistivity zone, it is wise not to ignore it. A drilling program to examine the existence of mineralized zones is recommended here too.

The IP anomaly around D-4-30, which was found in the SIP survey line "B", is on the serpentine body, coincident with a good geochemical anomaly, and is in the deep extension of the D-4-44 zone. It is expected to be caused

by nickel sulphides associated with serpentines, and it is recommended that a drilling program be conducted to examine the existence of mineralized zones.

Fig. Ⅲ-1 Compilation Map of CSAMT, SIP results, Geology & Geochemistry

PART 4
CONCLUSIONS AND RECOMMENDATION

CHAPTER 1. CONCLUSIONS

Based on the results of the first year program, four blocks, Areas C, D-1, D-2, and D-3, were selected for the second year program which employed modern geophysical methods, CSAMT and SIP. The purpose of the second year program was to examine the possibility of the existence of subterranean mineralized zones in the area by clarifying their geophysical properties.

The results of the second year program are as follows.

1. The CSAMT survey covered the whole 21km^2 area using 300m survey grid. A total of 306 survey points were measured. The following low resistivity zones (below 10 ohm-meter) were detected.

Area C;	C-80-3 to C-90-0, C-89-6, C-86-6, C-82-9
Area D-1;	D-43-9 to D-41-6, D-38-6 to D-36-6, D-31-9 to D-29-9
Area D-2;	D-8-18, D-4-9
Area D-3;	D-9-45, D-7-39, D-4-33, D-4-45

From them, Zones in favourable geological settings accompanied by good geochemical anomalies were selected for further SIP survey. Selected SIP survey lines and target anomaly zones were as follows.

SIP Survey Line "A"	D-8-18, D-7-39
SIP Survey Line "B"	D-4-33, D-4-45
SIP Survey Line "C"	D-38-6 to D-36-6
SIP Survey Line "D"	D-31-9 to D-29-9

2. The SIP survey was conducted to find IP effects and spectral phenomena caused by sulphide minerals. Survey Line "A" (4km, 160 measuring points), Survey Line "B" (3km, 80 measuring points), Survey Line "C" (1.5km, 30 measuring points), and Survey Line "D" (1.5km, 30 measuring points) were established.

Good IP anomalies were detected in the following zones.

SIP Survey Line "A"	D-7-7 to D-7-12, D-7-19 to D-7-23, D-7-30 to D-7-41
SIP Survey Line "B"	all over the deep position, but stronger at the both ends.
SIP Survey Line "C"	D-36-4 to D-36-8
SIP Survey Line "D"	D-30-6 to D-30-11

It is suggested that these anomaly zones are caused by some sulphide minerals, probably of, nickel sulphides associated with serpentines.

CHAPTER 2. RECOMMENDATION FOR THE THIRD YEAR PROGRAM

The results of the geological, geochemical, and geophysical survey programs for anomalous zones listed in CHAPTER 1. CONCLUSIONS strongly suggest that they are caused by nickel sulphides of the same type of ore as the Trojan deposits. A drilling program is therefore recommended for the next year's program to examine the existence of actual ore deposits. Among them, specially the zones of D-7-30 to D-7-41, D-4-43 to D-4-44, and D-37-4 to D-37-8 are evaluated as the first priorty targets.

REFERENCES

1) CHARLES, M. and SWIFT, JR (1971)
..... Theoretical magnetotelluric and turam response from two-dimensional inhomogeneities: Geophysics, V.36, P.38-52

2) GOLDSTEIN, M.A. (1971)
..... Magnetotelluric experiments employing an artifical dipole source: Ph. D. thesis, University of Toronto

3) GOLDSTEIN, M.A. and STRANGWAY, D.W. (1975)
..... Audio frequency magnetotellurics with a grounded electric dipole source: Geophysics, V.40, p. 669-683

4) METAL MINING AGENCY of JAPAN (1979)
..... Report of Mineral Resources Exploration Technology (1979, Development of Deep Electrical Exploration Technique)

5) METAL MINING AGENCY of JAPAN (1980)
..... Report of Mineral Resources Exploration Technology (1980, Development of Deep Electrical Exploration Technique)

6) METAL MINING AGENCY of JAPAN (1981)
..... Report of Mineral Resources Exploration Technology (1981, Development of Deep Electrical Exploration Technique)

7) METAL MINING AGENCY of JAPAN (1982)
..... Report of Mineral Resources Exploration Technology (1982, Development of Deep Electrical Exploration Technique)

8) METAL MINING AGENCY of JAPAN (1983)
..... Report of Mineral Resoruces Exploration Technology (1983, Deevelopment of Deep Electrical Exploration Technique)

9) NABETANI, S. and RANKIN, D. (1969)
..... An inverse method of magnetotelluric analysis for a multilayered earth: Geophysics, V.34, P.75-86

10) NELSON, P.H. (1977)
..... Induced polarization effects from grounded structures: Geophysics, V.42, P.1241-1253

11) PELTON, W.H., WARD, S.H., HALLOF, P.G., SILL, W.R. and NELSON, P.H. (1978)
..... Mineral discrimination and removal of inductive coupling with multifrequency IP: Geophysics, V.43, P.588-609

12) STRANGWAY, D.W., SWIFT, C.M. and HOLMER, R.C. (1973)
..... The application of audio-frequency magnetotellurics (AMT) to mineral exploration: Geophysics, V.38, P.1159-1175

13) SUMNER, J.S. (1976)
..... Principles of induced polarization for geophysical exploration, Elsevier Scientific Publishing, Amsterdan

14) SANDBERG, S.K. and HOHMANN, G.W. (1982)
..... Controlled-source audiomagnetotellurics in geothermal exploration: Geophysics, V.47, P.100-116

15) VAN VOORIS, C.D., NELSON, P.H. and DRAKE, T.L. (1973)
..... Complex resistivity spectra of porphyry copper mineralization: Geophysics, V.38, P.49-60

16) WYNN, J.C. and ZONGE, K.L. (1975)
..... EM coupling, its intrinsic value, its removal and the cultural coupling problem: Geophysics, V.40, P.831-850

17) YOKOKAWA, K., TSUJIMOTO, T., ENDO, Y. (1982)
..... Example of Cupling phenominan for spectral IP survey Butsuri-Tanko V.35, P.251-261

18) YOSHIKAWA, H., YOKOYAMA, T., YOKOKAWA, K., HOSOI, Y. (1980)
..... Spectral IP method: Butsuri-Tanko, V.33, P.287-293

19) ZONGE, K.L. and WYNN, J.C. (1975)
..... Recent advances and applications in complex resistivity measurements: Geophysics, V.40, P.851-864

20) ZONGE ENGINEERING & RESEARCH ORGANIZATION, INC. (1982)
..... Interpretation Guide for CSAMT Data